Preparation of Nanochitin by Break Down and Bottom-up Approaches

June 2022

Dagmawi Abebe Zewude

Department of Chemistry and Biotechnology

Graduate School of Engineering

Tottori University

Contents

List of Figures

List of Table

General introduction

Chitin is the major structural component of the exoskeleton of the crustaceans, crab shells, and shrimps. It is second most abundant polysaccharides, next to cellulose, found in nature. The annual synthetic amount is estimated to be 10^{10}–10^{11} tons.[1] Chitin, Poly-(1,4) linked 2-acetamido-2-deoxy-β-D-glucose, can be regarded as derivative of cellulose with the replacement of C-2 hydroxy group by an acetamide group.[2] Properties and chemical modifications of chitin mainly influenced by acetamide and hydroxy groups. This functional group with linear structure linked by hydrogen bond is responsible for its crystalline characteristics and chemical derivatization. Based on chain packing and hydrogen bonding, chitin can be distinguished into α, β, and γ polymorphic form.[2,3] Of these, α-chitin is by far most abundant.[4] α-chitin derived from crab shell exists as hierarchically arranged nano-size fibers in an antiparallel fashion. Chitin has attracted considerable attention due to its biodegradability, biocompatibility and biofunctionality.[5] However, its close packing through several inter and intra-molecular hydrogen bonds has limited the solubility of chitin in common solvent and dispersibility in water. Thus, it is difficult to process and commercialize. Most of the generated biomass is discarded as waste without any significant utilization.

Chitin can be changed into nano-sized material by downsizing method. The method and technologies of nanocellulose can be effectively used in the preparation of nanochitin as well. Powerful crushing equipment breaks the hydrogen bond and individualize chitin.

Derivative of nanochitin called partially deacetylated nanochitin prepared by removing some of the acetyl group from the surface of chitin by sodium hydroxide. This process changes the acetamide group ($-NHCOCH_3$) that exists at C2 position into amine group ($-NH_2$). Reducing the pH cationizes the amine functional group ($-NH_3^+$), which causes electrostatic repulsion and osmotic effects. This in turn, allows easy individualization and provides a characteristic of being completely dispersed in acidic water.

Bottom-up method is the other technique that can be used to prepare nanochitin. In this technique chitin is dissolved and regenerated again by using chemicals. Because of the difficulties in dissolving chitin in common solvent, the reports on the production of nanochitin by bottom-up method is very limited. Most of the reports are focused on chitosan, since it can be dissolved in acidic solution. Few report indicates that solvents including N,N-dimethyl acetamide/LiCl,[6] NaOH/urea,[7] alkaline-freezing,[8] and NaOH-ice,[9] has a potential of dissolving chitin. Kadokawa et al. successfully dissolved and regenerated chitin nanowhisker by using AMIMBR and methanol.[10]

Various applications of nanochitin were already clarified. For instance, chitin can be used to heal wound,[11] suppress skin inflammation,[12] promote hair growth,[13] relief from inflammation on the intestinal tract.[14] Different commercial products, which contains nanochitin as a functional material, such as skin care products and healthy foods are available in the market.

In this study nanochitin was prepared by using breakdown and bottom-up approach. For individualization of chitin low power generating ultrasonic and ball milling machine was used. The energy generated from this machine was able to break the hydrogen bonds connecting nano-sized fibers. The former was used for the case of partially deacetylated chitin and the later was used for non-deacetylated chitin under neutral condition. Bottom-up approach was used as another method of generating nanochitin. Surface deacetylated and non-deacetylated nanochitin was prepared. Sodium hydroxide was used to dissolve chitin and then regenerated it with acetic acid. The obtained nanochitin was characterized in terms of morphology, transparency, viscosity, chemical and crystalline structure. The downsizing and bottom-up method provided nanochitin with different size, morphology, physical, and chemical characteristics. The preparation technique employed in this experiment is very simple, cheap, and less energy consuming. Environmental, technical, and financial feasibility of producing nanochitin was given special attention.

In chapter 1, optimization of process parameters and preparation of partially deacetylated nanochitin using low power ultrasonic energy generating machine was described. The electrostatic repulsion that was initiated by dispersing partially deacetylated chitin into acetic acid containing water has enhanced the nanofibrillation process. Implosion of microbubbles generated by ultrasound releases energy, which creates mechanical impact on the suspended fiber. This energy was able to perform individualization. The ultrasonic frequency was optimized based on yield, physical, and chemical properties. Crystallinity and chemical structure were not affected by the ultrasonication process. By considering the

characteristics of the partially deacetylated chitin nanofiber and yield, 45kHz and 20 min treatment time was decided to be the optimum point.

Chapter 2 explains about the determination of optimum condition for the preparation of chitin nanofiber by ball milling process. Since polarity of the solvent determines the surface that interact with, water as polar solvent interacted with hydrophilic group (-OH) containing surface of chitin crystal faces and made the impact of ball milling efficient. Milling ball size, weight and time was significantly influenced the nanofibrillation process. The desperation property, morphology, size, and transparency were evaluated. Increasing ball weight has affected the crystallinity of the chitin.

In chapter 3 a novel method of producing chitin nanoparticle by bottom-up technique was explained. α-chitin was disentangled by soaking in concentrated NaOH solution and mixing with ice. This treatment changed the suspension into clear and viscous solution by breaking the inter and intramolecular hydrogen bonding. Addition of acetic acid was able to assemble the chains again by reforming the hydrogen bonds. The employed procedure has provided relatively uniform and thermally stable nanoparticles. The produced chitin nanoparticle was characterized to be highly dispersible in water, transparent, and lower viscosity compared to conventional chitin nanofiber. However, the crystallinity was observed to be low. In general, the preparation procedure and the characteristics of the nanochitin is much convenient than the conventional process for industrial production.

In chapter 4 energy saving and greener method was introduced to prepare uniformly shaped partially deacetylated chitin nanoparticle. In this process, chitin was treated with NaOH twice. In the first case, the acetyl group of chitins was partially removed by treating with NaOH at a temperature of 90 ^{0}C. This chemical modification has raised the primary amino group on the fibril surface. The second treatment with addition of ice was able to dissolve completely by changing the hydroxy groups (-OH) attached to C-3 and C-6 into sodium alkoxide (-ONa). Chitin nanoparticle was regenerated by mixing the suspension with acetic acid. Because of the deacetylation process, the surface chemistry was slightly modified. Soaking in acidic water was able to impart electrostatic repulsion. Better transparency and smaller size were obtained when compared with non-deacetylated nanoparticle, chapter 3.

Chapter 1

Optimum preparation conditions for highly individualized chitin nanofibers using ultrasonic generator

1.1. Introduction

Chitin is the main component of crab and shrimp shells. It has a chemical structure like cellulose since it is a repeating structure of 2-acetamido-2-deoxy-β-D-glucopyranose. The annual synthetic amount is estimated to be 10^{10}–10^{11} tons, which is the second largest resource after cellulose.[1] However, most of the crab shells are discarded without effective utilization. This is due to the fact that chitin is difficult to process and commercialize on account of its low solubility and dispersibility in water and common solvents.

We have produced nano-chitin by mechanical crushing of chitin extracted from crab shells by utilizing the preparing technology of nanocellulose.[15] All-natural chitin is composed of nano-sized crystalline fibrils[16] and can be converted to nanochitin by downsizing with a strong mechanical load. Nanochitin can also be produced from shrimp[17] and mushrooms[18] Nanochitin is a fibrous substance with a width of 10–20 nm. Since it is a highly crystalline fiber, it has excellent physical properties.[19] It can be molded into a desired shape depending on the application due to its uniformly water-dispersible characteristics.[20,21] Moreover, we have elucidated various biological functions of nanochitin and its partially deacetylated derivatives. For example, effects on the skin, a wound healing effect,[11] a relief effect of dermatitis,[12] and a hair growth effect[13] have been clarified. As an effect associated with taking the nanochitin, a relief effect of inflammation on the intestinal

tract[14] and anti-hepatic and antioxidative effects[22] have been demonstrated. By utilizing various functions, various commercial products containing nanochitin as a functional ingredient have been available such as cosmetics, skin care products, and healthy foods.

Powerful crushing equipment such as grinder and high-pressure homogenizer are often used to downsize chitin. The former equipment crushes chitin by the strong shearing force generated from two rotating grindstones.[15] The latter equipment crushes chitin by colliding a sample ejected at a high pressure from a nozzle.[23] These powerful equipment are needed to break the strong hydrogen bonds between chitin fibrils.

As a derivative of nanochitin, there is a partially deacetylated chitin nanowhisker.[24] This derivative is mostly deacetylated on the chitin surface by sodium hydroxide. The amino group at the C2 position on the partially hydrolyzed chitin is densely cationically charged under acidic conditions. Its cationic property brings electrostatic repulsion and osmotic effects, allowing nanowhiskers individualization and stable dispersion.

There is an ultrasonic generator as a kind of crushing device. Ultrasound initiates compression and rarefaction cycle. During the rarefaction, micro vacuum bubbles are created at various nucleation site, which then implode in the next high-pressure phase. It is a continuous formation of growth and implosion with a release of energy stored within the vacuum bubble.[25] The collapsing bubble creates a mechanical impact on the suspended chitin in the form of shock energy and length wise stress.[26] If the impact energy exceeds the force that binds the nanochitin together, they can break down in the form of nanofibers. The

efficiency of this process is strongly influenced by ultrasonication frequency and particle size.[27,28]

In this study, an ultrasonic generator with a variable frequency was applied to prepare partially deacetylated nanochitin. The equipment applied is commonly used for cleaning glassware with low power. The cationic charge on the surface of the chitin fibrils may allow for the disintegration of chitin by the cheap ultrasonic generator. The optimum ultrasonic frequency and treatment time were determined from the results of yield, shape, and physical and chemical properties to obtain the partially deacetylated nanochitin effectively. The production of nanochitin using an ultrasonic generator has already been reported.[29] However, in previous studies, chitin without deacetylation was treated with a high-power device for cell disruption at a constant frequency. The mechanical treatment using an ultrasonic generator with low power is characterized by its low acquisition cost, low energy consumption, and by being contamination-free. If partially deacetylated nanochitin are easily prepared by using it, the practical uses of chitin as a functional ingredient may increase.

1.2. Materials and methods

1.2.1. Materials

Chitin powder from crab shell was purchased from Koyo Chemicals Industry Co., Ltd. (Hyogo, Japan). The degree of deacetylation was 6%. Sodium hydroxide and acetic acid were purchased from Wako Pure Chemical Industries, Ltd. (Osaka, Japan) and used as received.

1.2.2. Partial deacetylation of chitin

Partially deacetylated chitin was prepared referring to the previous report with slight modifications.[24] In the process, α-chitin (45 g) was suspended in a 30 wt% NaOH aqueous solution (1,500 g) and the suspension was heated at 90 ^{0}C for 12 h with continuous stirring. After deacetylation, the precipitate was collected and washed repeatedly by a centrifuge until the supernatant became neutral with the rotational speed of 10,000 rpm for 10 min. A portion of the obtained product was kept for determination of degree of deacetylation and the rest was dispersed in a 1 wt% acetic acid aqueous solution. The degree of deacetylation of the partially deacetylated chitin was determined by the electroconductivity titration method.[24] 0.1 mol L^{-1} HCl was added to the chitin slurry to adjust the pH to 2.8, and 0.1 mol L^{-1} NaOH solution was added at 0.3 flow rate of mL min^{-1} up to pH 11. The conductivity and pH curves reflected the degree of deacetylation of chitin.

1.2.3. Ultrasonic treatment of partially deacetylated chitin

Partially deacetylated α-chitin slurry was stirred for six days for agitation followed by adjusting the solid content to 0.55 wt% using 1 wt% acetic acid. The obtained suspension, 200 g for each run, was transferred into 500 mL glass beaker and stirred for 30 min under a vacuum to remove air bubbles. Then, the suspension was subjected to ultrasonication process, using three frequency ultrasonic cleaner (VS-100 III, AS ONE, Osaka, Japan) in

water bath under stirring. Ultrasonic frequencies were 28, 45, and 100 kHz, and sonication times were 5, 10, 15, 20, 25, and 30 min. After sonication, large chitin fibers were removed

by centrifuging. The yield of partially deacetylated chitin nanofibers dispersed in the supernatant were gravimetrically calculated.

1.2.4. Characterizations of partially deacetylated chitin nanofibers

1.2.4.1. Morphological observation

Field emission scanning electron microscope (FE-SEM, JSM-6700F, JEOL, Tokyo, Japan) was used to ascertain the morphology of different partially deacetylated chitin nanofibers. Cast film was prepared and coated with an approximately 2 nm Pt layer by using an ion sputter coater and observed at 2.0 kV.

1.2.4.2. Determination of width of the nanofiber

Atomic force microscopy (AFM, Nanocute, SII Instruments, Chiba, Japan) was used to measure the width of nanofibers. Diluted chitin nanofiber dispersion was dropped on freshly cleaved mica substrate, dried at room temperature, and subjected to AFM observation. The widths of chitin nanofibers were measured by selecting the measuring points along the fiber axes.

1.2.4.3. Particle size and zeta potential measurement

Particle sizes and zeta-potentials of the partially deacetylated chitin nanofibers dispersed in water were measured using dynamic light scattering method (ELSZ-1000ZS, Otsuka Electronics, Osaka, Japan). The concentration of the dispersion for particle size and zeta potential measurement was 0.01 wt% and 0.005 wt%, respectively, at a pH of 3.

1.2.4.4. Crystalline structure and crystallinity index determination

X-ray diffraction profile of the chitin nanofiber was obtained in the range of $5^0 \leq 2\theta \leq 35^0$ by using Ni-filtered CuKα from an X-ray generator (Ultima IV, Tokyo, Rigaku) operating at 40 kV and 30 mA. The dry sample was prepared by freeze drying and then pressing into flat sheet at pressure of 20 MPa to generate the profile. Crystallinity index (CI) was determined based on the equation: $CI = (I_{110} - I_{am}) \times 100/I_{110}$, where I_{110} is the maximum intensity of the 110 plane and I_{am} is the intensity of the amorphous diffraction at 16^0.[30]

1.2.4.5. Viscosity and light transmittance measurement

Viscosity of the partially deacetylated chitin nanofiber suspension was measured by a Brookfield digital viscometer DV-E using spindle no. LV-4 (Brookfield Engineering Laboratories, Middleboro, MA, USA) after raising the solid content to 0.60 wt% by using a rotary evaporator.

The light transmittance of partially deacetylated chitin nanofiber dispersion with 0.1 wt% was measured using a UV-Vis spectrophotometer (V550; JASCO, Tokyo, Japan). The spectra were recorded in the range of 200 to 800 nm.

1.3. Results and discussion

1.3.1. Ultrasonic treatment of partially deacetylated chitin with different frequency

The deacetylation of chitin with 30 wt% NaOH at 90 ^{0}C for 12 h raised the degree of deacetylation to 36%. This value is reasonable compared to previous studies.[24] The amino group of partially deacetylated chitin is protonated under acidic conditions ($–NH_3^+$).

Positively charged chitin easily swells by electrostatic repulsive force and osmotic effect, resulting in facilitation of ultrasonication. Partially deacetylated chitin was treated with an ultrasonic generator. The frequencies are 28, 45, and 100 kHz. At frequencies of 28 and 45 kHz, the partially deacetylated chitin became a clear dispersion. This suggests that chitin was disintegrated to the nano level by ultrasonic waves, and the nano-sized chitin was individualized and dispersed in water. The ultrasonic generator brings ultrasonic vibrations to the water. The pressure difference due to vibration generates fine bubbles, which gives an impact to chitin and crushes it. During the ultrasonic treatment, low speed mechanical stirring of the chitin suspension is important. The efficiency and reproducibility of the ultrasonic wave impact on the chitin is improved by stirring at 65 rpm.

The disintegration efficiency was strongly dependent on ultrasonication frequency and treatment time. A higher yield was registered for 45 kHz followed by 28 kHz, as shown in Figure 1. When the ultrasonication minute was increased to 30, proportionally the yield was raised to 96%, in the case of 45 kHz. At a frequency of 28 kHz, the maximum yield obtained was 67% in 30 min of processing. A further increasing of frequency to 100 kHz did not increase yield within 30 min of processing at all. The observed trend can be explained based on the effect of cavitation bubble dynamics on the individualization process. Frequency controls cavitation bubble size, the number of cavitation bubbles, and the implosion energy. The energy generated from the cavitation bubble increases with bubble size and with a decrease in ultrasonic frequency.[27] Bigger cavitation bubbles are produced at lower frequency or higher wavelength since the bubble experiences enough time of rarefaction to grow before they implode.[31] On the other hand, at higher frequency a

large number of bubbles with weak impact are created.[28,32] Therefore, at a frequency of 28 kHz, larger size and smaller number cavitation bubbles with strong implosion energy are created. However, in the case of 100 kHz, relatively higher number of bubbles and smaller size with weak impacts are created. Therefore, the optimum bubble size, number, and impact for efficiently crushing the partially deacetylated chitin are created at 45 kHz. Thus, we performed a characteristic analysis of partially deacetylated chitin crushed by ultrasonic waves at a frequency of 45 kHz. On the other hand, when the original chitin was used for comparison, chitin could not be dispersed in water even after 30 min of ultrasonic treatment at a frequency of 45 kHz. This suggests that a deacetylation pretreatment is required for efficient disintegration of chitin.

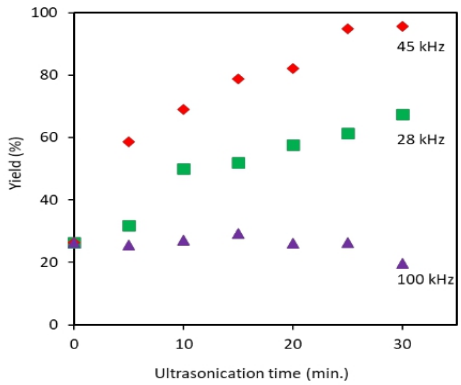

Figure 1. Dependence of yields on the ultrasonication frequency at 28, 45, and 100 kHz and ultrasonication time.

1.3.2. Morphological and structure characterization of partially deacetylated chitin nanofibers

FE-SEM images of partially deacetylated chitin ultrasonicated at a frequency of 45 kHz, which is the optimum frequency in yield are shown in Figure 2. The disintegrated product

obtained by ultrasonication was a spindle-shaped nanofiber with a width of about 10 nm and a length of several hundred nm. The nanofibers appeared to be uniform in width and length and to be smaller in width and length depending on the ultrasonic processing time, which will be described in detail later.

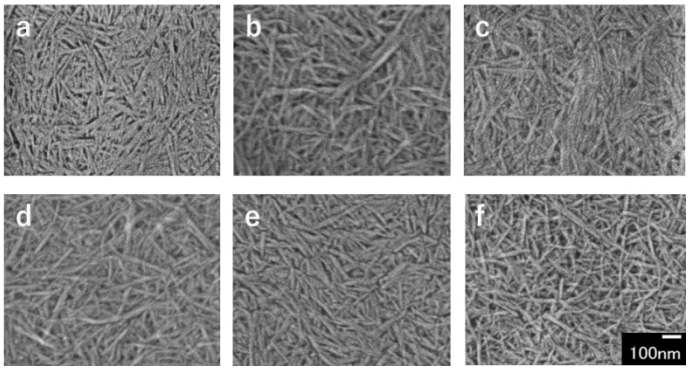

Figure 2. FE-SEM images of partially deacetylated chitin nanofibers with ultrasonication time of (a) 5, (b) 10, (c) 15, (d) 20, (e) 25, and (f) 30 min.

The AFM images of the nanofibers and the width distribution are shown in Figures 3 and 4, respectively. The shape of the nanofibers observed by AFM was in good agreement with the image by FE-SEM. The ultrasonication process at 45 kHz appears to reduce the width and length of the nanofiber. When the ultrasonic treatment time was 10 min or less, some nanofibers had a width of 10 nm or more. As the processing time increased, the width became smaller (from 4 to 5 nm was the most). Additionally, the fiber width distribution became narrower. This is because nanofibers are being disintegrated by ultrasonic treatment.

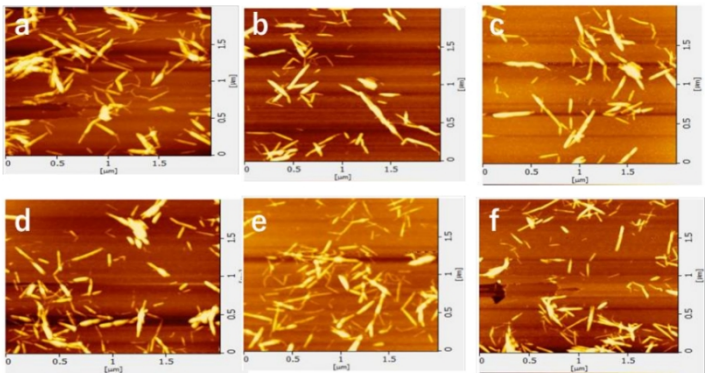

Figure 3. AFM images of partially deacetylated chitin nanofibers with ultrasonication time of (a) 5, (b) 10, (c) 15, (d) 20, (e) 25, and (f) 30 min.

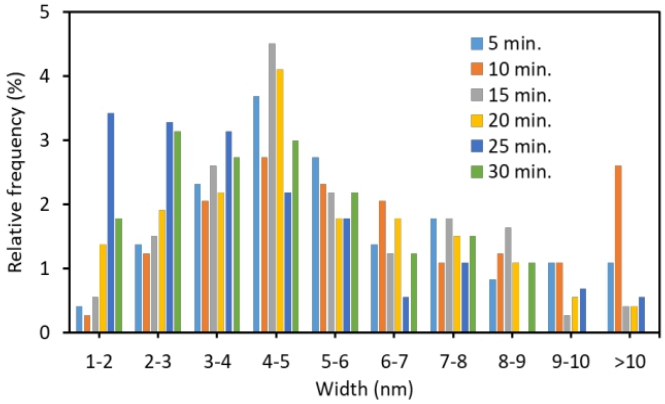

Figure 4. The effect of ultrasonication time at 45 kHz on the distribution of partially deacetylated chitin nanofiber.

The hydrodynamic diameter and its distribution were obtained by the dynamic light scattering method (Figure 5). The nanofiber rotates in water by Brownian motion, and the particle size correlates with the length of the nanofiber. We also evaluated the degree of dispersion, which is an index of uniformity from the particle size distribution. When the ultrasonic treatment time was 0 min, coarse particles having a particle diameter of 10,000 nm or more were observed. However, after ultrasonication for 5 min, the coarse particles

were completely disintegrated into fine nanofibers. When the treatment time was increased from 5 min to 15 min and 20 min, the disintegration further progressed, the particle size became smaller, and the distribution became narrower. Table 1 shows mean average size, and crystallinity index of partially deacetylated α-chitin nanofiber. When the treatment time was 0 min, the average particle size was 2025 nm but decreased to 629 nm after 5 min. of treatment. By increasing the sonication time, the average particle size decreased.

However, after the treatment for 20 min it almost leveled off. The polydispersity index was 0.78 when the sonication time was 0 min, but significantly reduced to 0.35 after 5 min treatment. The polydispersity index decreased slightly as the sonication time increased. Consequently, ultrasonication at a frequency of 45 kHz converts partially deacetylated chitin into nanofibers. The length and width changed depending on the processing time. The morphology of chitin nanofiber when sonicated at frequency of 45 kHz for more than 20 min shows good agreement with those reported in the past.[24]

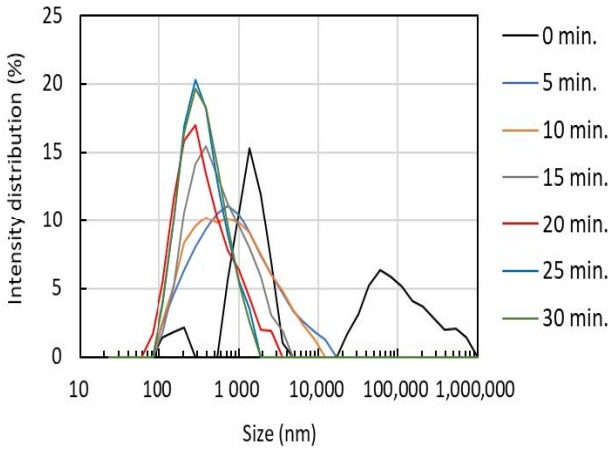

Figure 5. The effect of ultrasonication time on partially deacetylated chitin nanofiber size distribution.

Table 1. Mean average size, polydispersity index, and crystallinity index of partially deacetylated α-chitin nanofiber.

Ultrasonication Time (min)	Mean Average Size (nm)	Polydispersity Index	Crystallinity Index (%)
α-chitin powder	-	-	89.88
0	2025	0.78	89.73
5	629	0.35	87.02
10	549	0.35	86.31
15	429	0.29	85.37
20	310	0.32	87.87
25	309	0.29	87.05
30	294	0.26	87.05

The X-ray diffraction profiles of pure chitin, partially deacetylated chitin, and nanofiber with respective ultrasonication minute was used to investigate change in crystallinity (Figure 6). The diffraction profile of α-chitin in the range of $5^0 \leq 2\theta \leq 35^0$ shows more intense peaks located at $2\theta = 9.36^0$ and 19.28^0 which corresponds to (020) and (110) crystallographic plane. Less intense peaks can be observed at $2\theta = 12.80^0$, 20.91^0, 23.22^0, and 26.39^0 which associated with (021), (120), (130) and (013), respectively, and close to previous reports.[33,34] Relative crystalline index was determined from intense peak of 110 plane in the range $19^0 \leq 2\theta \leq 20^0$ and the amorphous diffraction at 16^0 .[30] As shown in Table 1, the relative crystallinity index of partially deacetylated chitin nanofibers treated with ultrasonic waves was about 87% regardless of the treatment time, which was almost constant. This suggests that sonication does not damage the crystalline region of chitin, (that is, it breaks the amorphous region). This result is consistent with previously reported studies.[24] In addition, the FT-IR spectrum of the partially deacetylated chitin nanofiber did not change depending on the processing time. This suggests that sonication does not alter the chemical structure of chitin (Figure 7)

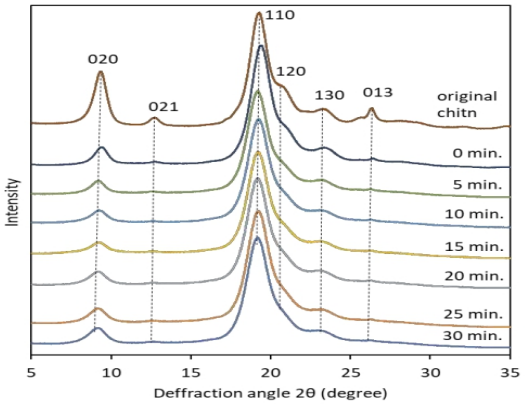

Figure 6. X-ray diffraction patterns of pure α-chitin powder and partially deacetylated α-chitin with different ultrasonication time.

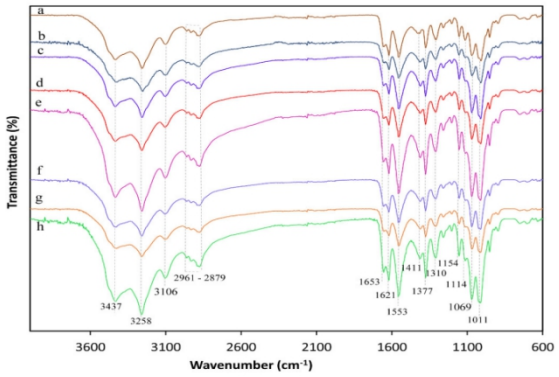

Figure 7. FT-IR spectra of pure α-chitin powder (a), partially deacetylated α-chitin (b), and ultrasonicated for 5 (c), 10 (d), 15 (e), 20 (f), 25 (g), and 30 min (h).

ζ-Potential of the partially deacetylated chitin nanofiber aqueous dispersion was measured. Figure 8 shows the ζ-potential when ultrasonicated for 5 to 30 min. Nanofibers had a cationic surface charge under acidic conditions. This is due to the protonation of the amino group ($–NH_3^+$) on the surface of the nanofiber. Thus, pH of the dispersion has a strong effect on the ζ-potential.[24] The electrostatic repulsive force between nanofibers with a cationic surface charge contributes to the dispersion stability in water. The ζ-potential of the nanofibers sonicated for 5 min had a high positive surface charge (+68 mV), and this

value was decreased with increasing the processing time. It is suggested that the surface area of the nanofiber is increased by the ultrasonic treatment and, as a result, the ionic strength is increased. At higher ionic strength, the shielding effect becomes strong. This shielding might have led to reduction in effective charge of the cations, so that there was a shrink in the slipping plane. That is, the higher cationic surface charge offsets the electrostatic repulsive force of the nanofiber in water. This may reduce the Debye length in addition to affecting shrink in slipping plane, resulting in an increase in Van der Waals force. According to the Derjaguin-Landau-Verwey-Overbeek (DLVO) theory, the total interaction energy is considered to be a combination of Van der Waals force and electrostatic force.[35,36] As the sonication time increased, the Van der Waals force increased and electrostatic force decreased, which suggests decrease of ζ-potential. The effect of decrease in ζ-potential was clearly shown on the viscosity of nanofibers as described below.

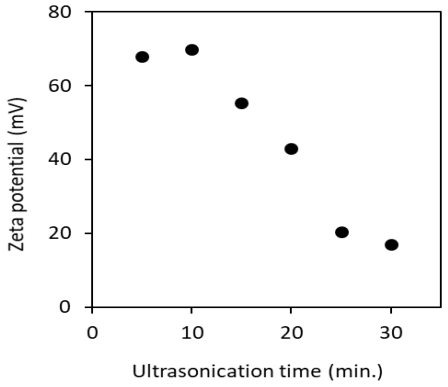

Figure 8. Zeta potential of partially deacetylated chitin nanofiber as a function of ultrasonication time.

1.3.3. Properties of partially deacetylated chitin nanofiber dispersion in water

The viscosity of partially deacetylated α-chitin nanofiber at a solid content of 0.60 wt% with different ultrasonication time is shown in Figure 9. Before ultrasonication, the viscosity of partially deacetylated chitin was relatively low (9.25 mPa·s). This is due to the fact that, before the ultrasonic treatment, the unindividualized partially deacetylated chitin fibers are thick and have a wide distribution, so that there is little entanglement between the fibers. After 5 min of sonication, the viscosity increased significantly, reaching 850 mPa·s. On the other hand, after 10 min or more of treatment, the viscosity decreased and became almost constant in 15 min. This is related to the morphology of the nanofibers. That is, chitin was converted into nanofibers by sonication and interacts with each other in water to increase its viscosity. On the other hand, sonication for 10 min or more shortens the fiber length. Shortening the nanofibers suppresses the entanglement of the nanofibers, resulting in a decrease in viscosity. The ζ-potential of nanofibers is also involved. That is, the fiber length decreases with the ultrasonic treatment. As disintegration progresses, new interface of chitin was appeared. Then, the ionic strength increases, and the ζ-potential decreases as described above. A decrease in ζ-potential reduces the interaction and dispersibility of nanofibers, resulting in a decrease in viscosity. Moreover, the decrease in ζ-potential reduces the electrostatic repulsive force of the chitin nanofibers, and then reduces the viscosity of the dispersion. From the above, it was found that the viscosity of the nanofiber can be controlled by the ultrasonic treatment time. The decrease in viscosity makes it possible to increase the concentration of nanofibers, which is industrially advantageous.

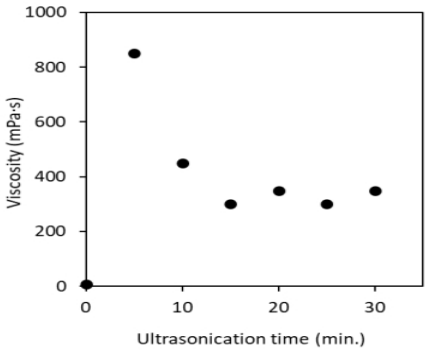

Figure 9. Viscosity of partially deacetylated chitin nanofiber suspension as function of ultrasonication time.

The UV-Vis transmittances of partially deacetylated chitin nanofiber with 0.1 wt% dispersion at different ultrasonication time were shown in Figure 10. The transmittance of the unsonicated partially deacetylated chitin dispersion was 78% at 600 nm, but the transmittance increased as the ultrasonic treatment time increased. This is clearly due to the nanofiber morphology. That is, sonication reduces the width and length of nanofibers and narrows their distribution. Such a change in morphology suppresses light scattering of nanofibers and improves transparency. In addition, the positive charge on the surface of the nanofiber promotes stable dispersion for a long period of time, enabling individual dispersion.

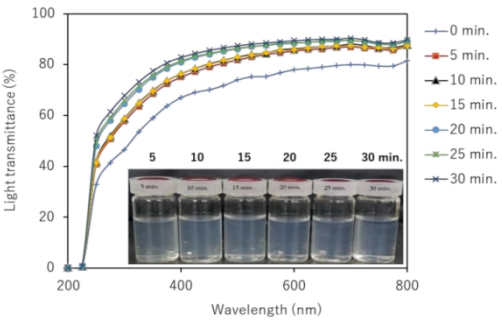

Figure 10. Photographs and UV-Vis transmittance spectra of partially deacetylated chitin nanofiber with respect to ultrasonication time and those photographs.

1.4. Conclusion

Partially deacetylated chitin could be disintegrated to the nano level using a commercially available ultrasonic cleaner. The positive charge of partially deacetylated chitin facilitates downsizing, also allows for a high dispersibility. The highest yield of ultrasonic waves was achieved at 45 kHz, reaching 96% after 30 min of treatment. On the other hand, at 100 kHz, it could not be downsized at all. The sonicated chitin was a nanofiber individualized and homogeneously dispersed in water. The fiber width and length can be controlled by changing the processing time. The fiber width of the nanofiber treated for 30 min was about 4–5 nm, and the average fiber length was 294 nm. Therefore, the aspect ratio was estimated to be about 60–70. Ultrasonic cleaners can be purchased inexpensively and consume less power. Partially deacetylated chitin nanofibers have excellent physiological functions. The results of this study will lead to clinical research on partially deacetylated chitin nanofibers and promotion of their use as pharmaceuticals and medical devices.

Chapter 2

Optimization of chitin nanofibers preparation by ball milling for fillers in composite resin

2.1. Introduction

Chitin is a polysaccharide with a chemical structure similar to cellulose with N-acetylglucosamine as the repeating unit. It is synthesized as a structural material by a variety of organisms, including the outer shells of crabs, shrimp, and insects, and the cell walls of molds, mushrooms, and diatoms, and is known as the second most abundant biomass after cellulose. However, it is rarely used except for some medical materials, compared to the large industrial use of cellulose and its derivatives in the paper, fiber, and food applications. This is because chitin is insoluble in common solvents, making it difficult to process. Using cellulose nanofiber production technology,[37] we have developed a technology to prepare chitin nanofibers from crab shells.[15] Chitin nanofibers have a uniform shape with a width of approximately 10 nm and are easily processed because they are obtained as a uniform water dispersion. Several forms have been obtained by dehydration of aqueous dispersions of chitin nanofibers. For example, the threads have been produced by spinning,[38] paper sheets by filtration,[39] and sponges by freeze-drying.[40] Because it is a water dispersion, it is easier to evaluate its functionality, and *in vitro* and *in vivo* studies have revealed various physiological functions. For example, we have identified their effects when applied to the skin,[11,13] taken,[22,41] or administered to plants.[42,43] Utilizing those functions, healthcare-related products containing nanofibers have been commercialized. Other applications include reinforcing fibers to strengthen materials.

Chitin nanofibers are crystalline materials consisting of linear chitin molecules regularly arranged by hydrogen bonds and thus have excellent mechanical properties.[44,45] Plastics composited with chitin nanofibers have been reported.[19] The reinforcing effect of chitin nanofibers significantly increased the strength and modulus of elasticity of the plastic and reduced its thermal expansion.[46] In addition, the plastic maintained high transparency despite the high content of nanofibers. This is due to the size effect of nanofibers. That is, when their width is sufficiently smaller than the wavelength of visible light, the light is hardly scattered in the composite.

Purified chitin can be mechanically pulverized in water to prepare chitin nanofibers. This is because the chitin in crab shells is composed of nanofibers.[47] That is, numerous chitin molecules assemble to form crystalline nanofibers. The chitin nanofibers form a complex with proteins, and their higher-order structures are organized into crab shells. The voids are filled with calcium carbonate. Since all natural chitin exists as nanofibers, chitin from various sources such as shrimp shells[17] and mushrooms[18] can be converted to nanofibers. In addition, since natural chitin is an aggregate of nanofibers, chitin can be converted to nanofibers using a variety of milling machines. The nanofibers have been produced using a millstone grinder,[48] a high-pressure homogenizer,[23] and a high-speed blender.[49] These are breakdown-type methods in which micro-sized samples are pulverized and converted to nano. Therefore, it is important to note that the shape of the chitin nanofibers obtained depends on the pulverization condition, which can significantly change the physical properties of the dispersion and the molded product.[50] One of the typical milling machines is the ball mill. In a ball mill, hard balls are placed in a cylindrical container and rotated,

causing the balls to move at high speed and grind the sample with impact and friction. Ball mills are relatively inexpensive as milling machines, have low energy consumption, the degree of milling can be easily controlled depending on conditions, and they are batch-type mills that can be used for milling small amounts. Therefore, the ball mill is expected to be one of the production devices for chitin nanofibers. Although, there have been several related reports,[51-53] there have been no studies on the direct preparation of aqueous dispersions of chitin nanofibers by wet processing using a ball mill. Therefore, this study attempted to produce chitin nanofibers by ball milling to develop a new production method for chitin nanofibers. Optimal conditions for efficient production of chitin nanofibers were verified by milling with different ball sizes, total ball volume, and milling time, and analyzing the resulting milled fibers.

2.2. Materials and methods

2.2.1. Materials

Chitin powder from crab shell was purchased from Koyo Chemicals Industry Co., Ltd. and used as received. The degree of deacetylation was 6%.

2.2.2. Preparation of chitin nanofiber

Chitin was subjected to ball milling in Pulverisette 6 classic line (Fritsche Japan). The 60 g of chitin water dispersion (5 wt%) was put into a 500 mL zirconia container and zirconia balls were added. Milling was performed at a rotation speed of 300 rpm and stopped every 30 min for 15 min for cooling. Different milling conditions were used to study the effect of these factors, including ball size (0.3-20 mm), total ball weight (20-600 g), and milling time

(30-300 min). After milling, balls were removed from chitin by decantation and were rinsed with distilled water to collect chitin.

2.2.3. Preparation of chitin nanofiber cast film

8 g of milled chitin dispersion (1 wt%) was mixed with 10 g of acetone and stirred for 1 h under low pressure to remove air bubbles. The resulting mixture was poured into a Petri dish to dry at 35 ^{o}C for 36 hours. Thus, obtained cast film was used to measure the transparency and density.

2.2.4. Characterization of milled chitin dispersion and the cast film.

2.2.4.1. Morphological observation and size measurement

A field emission scanning electron microscope (FE-SEM, JSM-6701F, JEOL, Japan) was used to observe the morphology and measure the length of milled chitin. Before imaging, the sample was coated with an approximately 2 nm Pt layer by using an ion sputter coater and observed at the electron-acceleration voltage of 2.0 kV. The fiber lengths of chitin nanofibers were determined by measuring over 150 randomly selected nanofibers from each sample.

An atomic force microscope (AFM, Nanocute, SII Instruments, Chiba, Japan) was also used to observe and measure the width of the nanofiber. The diluted sample was dropped on the freshly cleaved mica substrate and dried at 35 ^{o}C overnight for observation. The fiber widths were determined by measuring over 150 randomly selected points along the fiber axes.

2.2.4.2. Crystalline structure and crystallinity index determination

The crystal structure was studied by using an X-ray generator (Ultima IV, Rigaku Corporation, Tokyo, Japan) with Ni-filtered CuKa radiation. The observation voltage and current were set at 40 kV and 40 mA, respectively. XRD sample was freeze-dried and then crushed using mortar and pestle. The crystallinity index (CI) was estimated from the X-ray profile using CI = (I_{110} -I_{am}) x 100/I_{110}, where I_{110} is the maximum intensity of the 110 plane at approximately 19^{o} and I_{am} is the amorphous diffraction intensity at 16^{o}.[30]

2.2.4.3. Light transmittance and viscosity measurement

The light transmittance of the milled chitin dispersion at a concentration of 0.1 wt% and the cast film was measured using a UV-Vis spectrophotometer (UV-2600i, Shimadzu Corporation, Japan). The spectra were recorded in the range of 300 to 900 nm.

The viscosity of the milled chitin dispersion at a concentration of 1 wt% was measured using Brookfield digital viscometer DV-E (Brookfield Engineering Laboratories, Middleboro, MA, USA) with spindle no. LV-3 and rotational speed of 6 rpm. The sample was kept in a water bath at a temperature of 30 ^{o}C for at least 45 minutes before measurement.

2.2.4.4. Determination of yield

To study the amount of fully milled chitin, the ratio of supernatant was measured as nanofiber yield. After milling, the chitin dispersion was diluted to 0.1 wt% by water and centrifuged at 1,000 rpm for 35 min to remove coarse microfiber, and concentrations before

and after centrifugation were compared. The supernatant was also used for microscopic observation.

2.3. Results and discussion

2.3.1. Influence of ball diameter

The optimum ball size for milling chitin was investigated. The total weight of the balls was fixed at 120 g and the grinding time at 120 min. Figure 11a shows the viscosity of the chitin dispersion when ground with balls of 0.3 to 20 mm in diameter. Viscosity correlates with the number of nanofibers produced by ball milling, specific surface area, and aspect ratio.[50] These parameters affect interactions such as intermolecular forces and physical entanglement between nanofibers. When the ball diameter was 20 mm, the viscosity was 150 mPa·s. The viscosity increased as the ball size decreased, reaching a maximum value of 300 mP·s at 1 mm. This was influenced by the specific surface area of the balls. For example, when the ball size changes from 20 mm to 5 mm, the number of balls with a total weight of 120 g increases from 5 to 286 balls, respectively, and their surface area increases significantly. Therefore, the frequency with which the balls collide with the chitin increases, resulting in more efficient grinding.[54] On the other hand, when the size was 0.3 mm, the viscosity decreased significantly to 140 mPa·s. The different result is presumably due to the impact force of the ball. The smaller ball size increases the surface area, while the lower weight per ball decreases the impact energy imparted to the sample, suggesting that the energy imparted by the 0.3 mm ball is insufficient for grinding chitin. Figure 11b shows the transparency of chitin dispersions milled with balls of different sizes. The transparency of the dispersion is strongly influenced by the shape and dispersibility of the chitin

nanofibers.[50] This is because well-milled chitin has a less diffuse reflection of visible light at the interface with water due to the nanosize effect. In addition, when the affinity between water molecules and nanofibers is high, aggregation between chitin is suppressed and uniform dispersion is achieved, resulting in improved transparency. In Figure 11b, the transmittance increased continuously as the ball size decreased, suggesting that the chitin is more pulverized. This is because, as already mentioned, when the ball size is reduced, the frequency of collisions with the chitin increases and the milling becomes more efficient. Figure 11c shows the yield of chitin nanofibers. Chitin contained in the supernatant solution of aqueous chitin dispersion after centrifugation was considered as nanofibers, and the yield was determined. Well-milled chitin nanofibers do not precipitate by centrifugation and remain in the supernatant because of their improved dispersibility in water. At a ball size of 20 mm, the yield of chitin nanofibers in the supernatant was 44%, but increased with decreasing size, reaching 62% at 1 mm. At 0.3 mm, however, the percentage decreased to 45%. This trend is in good agreement with that of viscosity since the impact by the 0.3 mm ball is insufficient to convert chitin into nanofibers, leaving coarse chitin fibers.

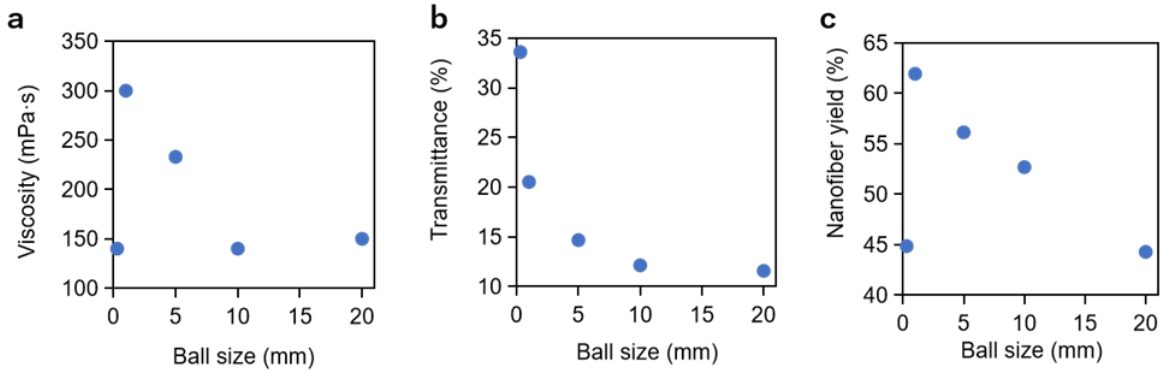

Figure 11. (a) Viscosity, (b) transmittance at 600 nm, and (c) nanofiber yield after milling of chitin using different ball sizes.

The transmittance at 600 nm and the density of cast films made with aqueous chitin nanofiber dispersion are shown in Figure 12. The transparency and density of the cast films are highly correlated with the degree of chitin pulverization.[23,50] Chitin is inherently a substance that absorbs little visible light, so its films can be transparent. Well-milled chitin nanofibers increase transmittance and density because they can be filled without gaps in the film after drying. On the other hand, coarse fibers with insufficient milling caused air voids in the film, thus reducing density. In addition, since air and chitin have very different refractive indices, a diffuse reflection of light occurs at the interface between them, reducing transparency. The results for transmittance and density of the cast film were in good agreement with those for the viscosity of the water dispersion and the percentage of supernatant. That is, the transmittance and density of the film increased as the ball size decreased, with the highest values at 1 mm. On the other hand, when the ball was 0.3 mm, the transmittance and density decreased. This supports the above discussion that ball size affects the frequency and grinding power of chitin grinding.

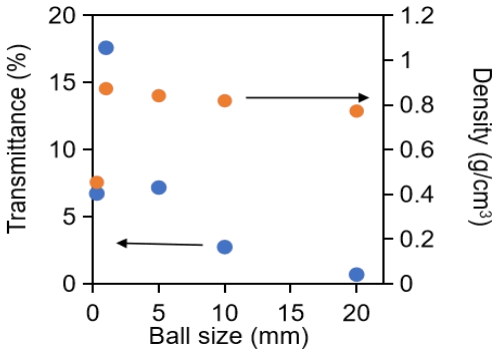

Figure 12. Dependence of transmittance at 600 nm and density of the cast film on different ball sizes for milling of chitin.

The distribution of nanofiber length and width obtained from the SEM and AFM images is shown in Figure 13. When the ball size was 1 mm, the distribution of nanofiber length was the narrowest and the average fiber length was the smallest. That is, there were few nanofibers longer than 700 nm. Fibers with lengths between 100 and 300 nm accounted for 56% of the total. Regarding the distribution of nanofiber widths, chitin treated with 1 nm balls was the most pulverized. Fibers with widths greater than 13 nm were the least abundant (4%), and finer nanofibers with widths of less than 5 nm and 5-7 nm were the most abundant (13% and 34%, respectively).

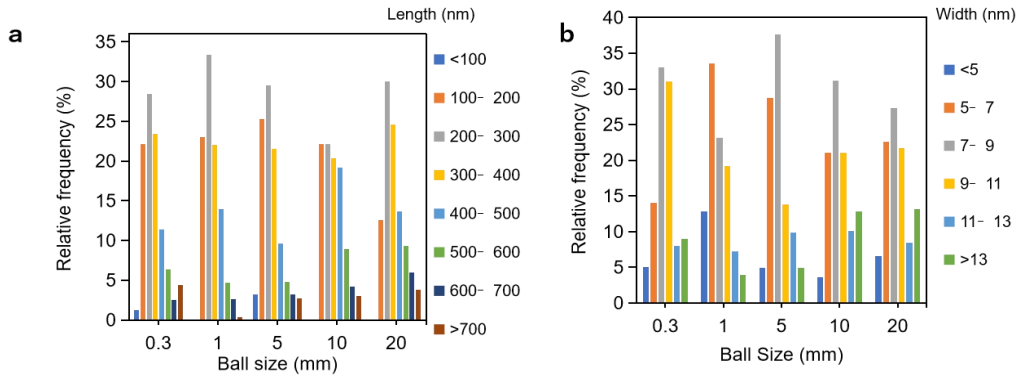

Figure 13. Distribution of (a) length and (b) width of chitin nanofibers milled at different ball sizes.

These results show that when grinding chitin in a ball mill, the size of the balls has a significant effect on the grinding of chitin. Reducing the size increases the surface area of the ball, which increases the frequency of chitin grinding. On the other hand, if the balls are too small, they are too light and therefore insufficient for their crushing. Thus, the optimal ball size for crushing chitin is 1 mm.

2.3.2. Influence of total ball weight

The optimal total ball weight for grinding chitin was investigated. Ball size and milling time were fixed at 1 mm and 120 min, respectively. The viscosities of the resulting aqueous chitin nanofiber dispersions are shown in Figure 14a when chitin was ground with balls with a total weight of 20 to 600 g. The viscosity, which was 140 mPa·s at a total ball weight of 20 g, increased as the ball weight increased, reaching a maximum value of 300 mPa·s at 120 g. This is because the total ball weight is proportional to the number of balls, thus increasing the frequency of chitin crushing. On the other hand, the viscosity decreased when the ball weight was above 300 g. This is presumably because excessive milling caused longitudinal cleavage parallel to the nano-fibrillation of the chitin, resulting in a decrease in aspect ratio. Shorter fibers decrease the viscosity of the dispersion. The transmittance of the nanofiber water dispersion is shown in Figure 14b. The transmittance was 15% when the total ball weight was 20 g and increased as the weight increased, reaching a maximum of 27% when the weight was 300 g. This is due to the increase in the number of balls and the frequency of milling as well as the viscosity results. On the other hand, when the weight was 600 g, the transmittance decreased (16%). The grinding mechanism of a ball mill grinds the sample in a rotating container by impact and friction as the balls move against the inner walls of the container. When there is an excess of balls in the container, the motion of the balls is restricted and interferes with the grinding of the sample. Indeed, when using 600 g balls, the volume of balls in a 500 ml container is estimated to be 90 cm^3, accounting for 18%. That percentage is larger than that of the aqueous chitin dispersion. The results are similar to those of the yield of chitin nanofibers

remaining in the supernatant (Figure 14c). As the total weight of the balls increased, the percentage of chitin in the supernatant increased, reaching a maximum when the total weight was 300 g, with a yield of 75%. On the other hand, at 600 g, the yield decreased to 45%. Excess balls reduce the efficiency of the milling process.

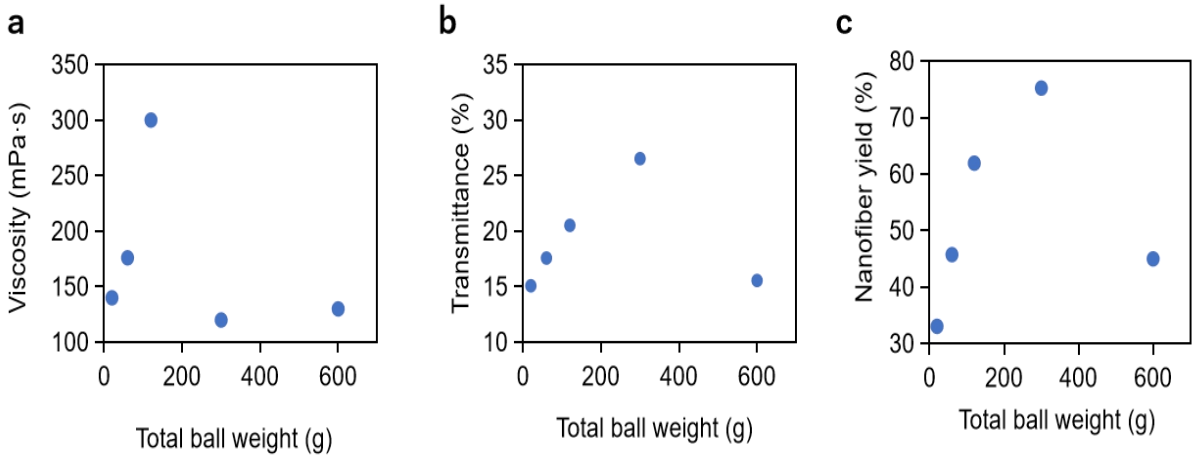

Figure 14. (a) Viscosity, (b) transmittance at 600 nm, and (c) nanofiber yield after milling of chitin using different total ball weights.

The transmittance and density of cast films prepared from aqueous nanofiber dispersion are shown in Figure 15. The trends in the transmittance and density of the films for different total ball weights correlate well with those of the aqueous dispersion. Specifically, as the total ball weight increased from 20 g to 300 g, the transmittance and density increased linearly from 2% to 55% and from 0.55 g/m^3 to 0.99 g/m^3, respectively. On the other hand, when the ball weight was 600 g from 300 g, they decreased to 9% and 0.75 g/m^3, respectively.

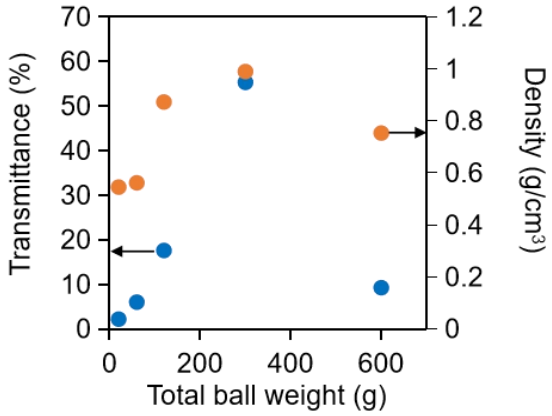

Figure 15. Dependence of transmittance at 600 nm and density of the cast film on different total ball weights for milling of chitin.

The distribution of length and width of nanofibers when milled with balls of different weights is shown in Figure 16. As the ball weight increased, the percentage of short nanofibers increased. For example, at a ball weight of 300 g, few fibers with lengths greater than 500 nm were present, while nanofibers with lengths of less than 100 nm and 100-200 nm were in the majority, at 11% and 36%, respectively. This indicates that the nanofibers are cut in the length direction by the balls. On the other hand, the width of the fibers tended to increase with ball weight. For example, when comparing the results for ball weights of 120 g, 300 g, and 600 g, the percentages of fibers with widths of 5-7 nm decreased to 33%, 17%, and 13%, respectively, while those with widths of 11 nm and above increased to 11%, 23%, and 31%. This may be due to changes in the crystallinity of chitin nanofibers.

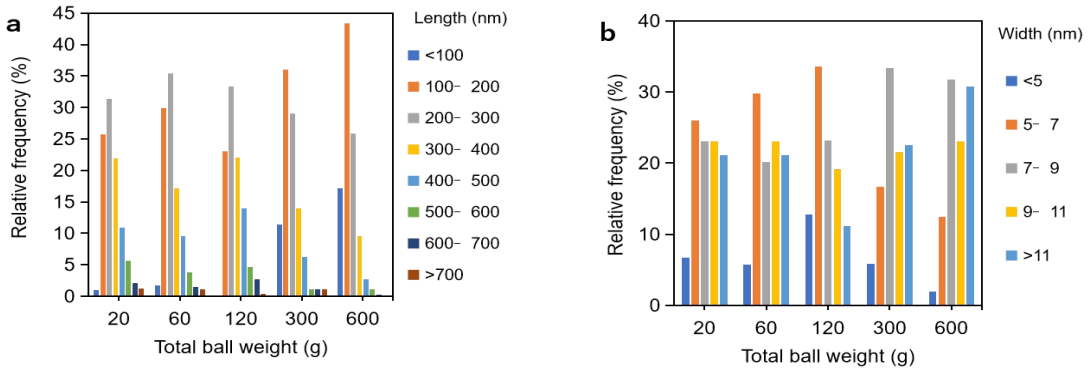

Figure 16. Distribution of (a) length and (b) width of chitin nanofibers milled at different total ball weights.

Therefore, to study the effect of total ball weight on the crystallinity of chitin, X-ray scattering measurements were performed and the relative crystallinity was determined from the profiles (Figure 17). The crystallinity of the raw chitin was 89.9% but decreased with ball milling. The crystallinity decreased slowly with the total weight of the balls, and at a ball weight of 600 g, the crystallinity was 61%. This suggests that the chitin crystals are being destroyed by the ball impact. Amorphization of crystalline chitin may be causing an increase in fiber width.

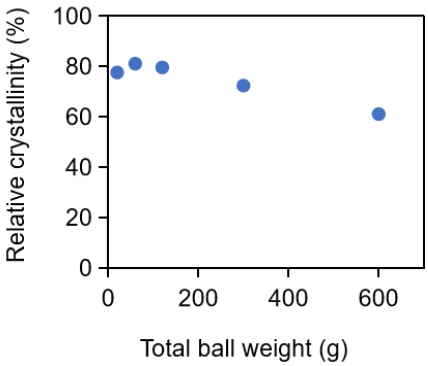

Figure 17. Dependence of relative crystallinity index of chitin nanofibers on total ball weight.

These results show that the total weight (or number) of balls has a significant impact on chitin crushing. As the total weight increases, there are more opportunities for chitin to be crushed, resulting in increased fineness. However, when the vessel is filled with an excess of balls, the movement of the balls is inhibited, and thus the efficiency of the milling process is reduced. Therefore, the appropriate total weight of the balls under these milling conditions was 300 g.

2.3.3. Effect of milling time

The effect of grinding time by ball milling on chitin was investigated. Based on the results of the above study, the ball size and total ball weight were fixed at 1 mm and 300 g, respectively. The viscosity of the aqueous dispersion when processed in the ball mill for 30 to 300 min is shown in Figure 18a. The viscosity was highest at 200 mPa·s when the total milling time was 30 minutes. This is due to the conversion of chitin into nanofibers by milling, which increases the interaction between the fibers. On the other hand, after 60 minutes of grinding, the viscosity decreased significantly to 110 mPa·s and the viscosity remained almost constant after further crushing. This suggests that the crushing process caused longitudinal cleavage parallel to the refinement of the chitin. A decrease in aspect ratio causes a decrease in viscosity. The transparency of the nanofiber dispersion is shown in Figure 18b. The light transmittance increased continuously with milling time. This suggests that the milling process refined the chitin fibers in the length and width directions, resulting in improved dispersion and suppression of optical scattering. However, after 240 minutes, the transmittance has almost reached a plateau. The yield of chitin nanofibers in

the supernatant of the dispersion is shown in Figure 18c. As the grinding time increased, the percentage of chitin increased significantly, reaching 75% after 120 minutes of grinding. Thereafter, however, the increase in chitin yield became moderate. These results suggest that the shape does not change significantly after a certain amount of milling time.

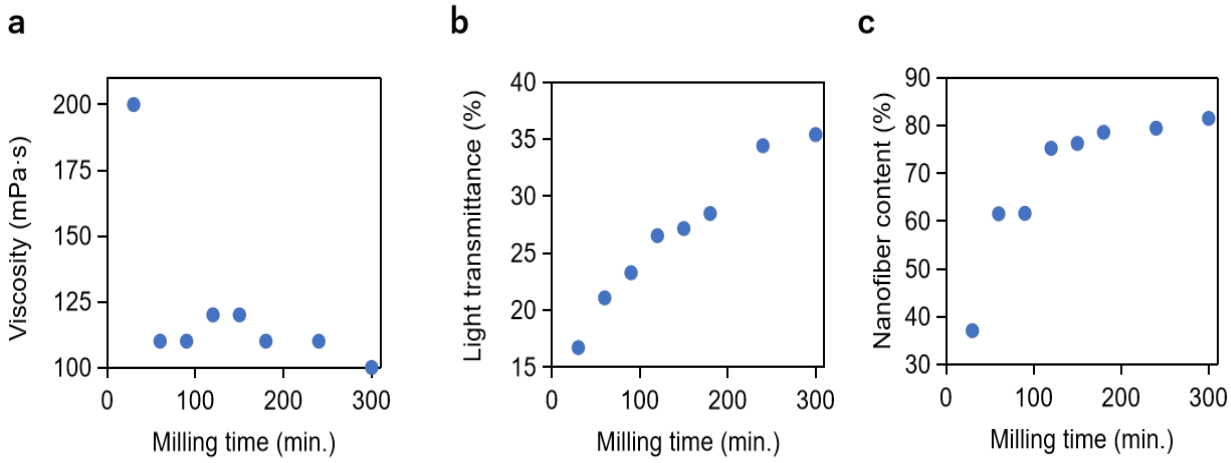

Figure 18. (a) Viscosity, (b) transmittance at 600 nm, and (c) nanofiber yield after milling of chitin with different milling times.

Such a trend of change in the physical properties of the nanofiber dispersion is also observed in the transmittance and density of its cast film (Figure 19). That is, the transmittance of the film increased with milling time. This suggests a progression of chitin refinement. The density of the film also increased with the progression. However, after 150 minutes of milling, the transmittance almost reached a plateau, and the same trend was observed for density.

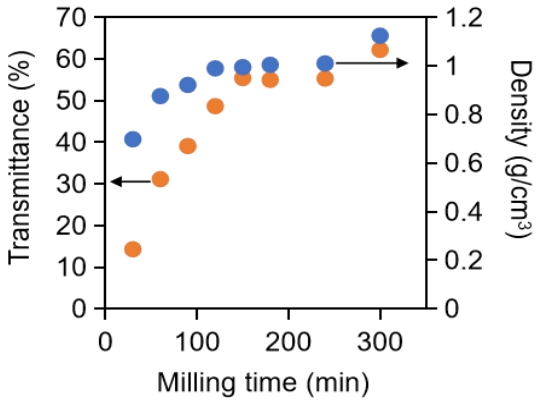

Figure 19. Dependence of transmittance at 600 nm and density of the cast film on milling time of chitin.

These results show that the nano-fibrillation of chitin progresses depending on the milling time, but the shape change converges after a certain amount of time. Therefore, the appropriate milling time was approximately 150 min.

2.4. Conclusion

Optimal conditions for producing chitin using a ball mill were identified. Ball size, total ball weight, and milling time have a significant impact on chitin milling efficiency. In other words, the morphology of the nanofibers and the viscosity and transparency of their dispersions and the yield of the nanofibers, and the transparency and viscosity of their cast films changed significantly depending on these milling conditions. Based on those results, the optimal conditions were determined to be a ball size of 1 mm, a total ball weight of 300 g, and a milling time of 150 minutes. Because of its excellent physical properties, chitin nanofiber is expected to be used as a reinforcing material to create nanocomposites. Technology for efficiently grinding chitin into nanofibers using less energy is important to promote the use of chitin nanofibers produced from underutilized resources.

Chapter 3

Production of chitin nanoparticles by bottom-up approach from alkaline chitin solution

3.1. Introduction

Chitin is the main component of crab and shrimp shells. The chemical structure of chitin with repeated linkage of *N*-acetylglucosamine is similar to that of cellulose. The amount of biosynthesis in nature is estimated to be second to that of cellulose, but its utilization is much smaller than that of cellulose. This is because chitin is insoluble in common solvents, making it difficult to process and verify its function. In recent years, nanochitin has been developed by applying the manufacturing technology of nanocellulose.[15,55] Compared with conventional chitin, nanochitin disperses uniformly in water, so it is easy to process and evaluate its function.[19,38] As a result, numerous biological functions of chitin nanofibers have been clarified. For example, the effect when applied to the skin,[11,13] taken,[22,41] and given to plants have been clarified.[42,43] Fibrous nanochitin can be obtained by mechanically crushing chitin in the same manner as cellulose. Since all natural chitins are aggregates of nanoscale chitin microcrystals,[47] they can be easily converted to nanochitin by a simple pulverization process.[17,18] However, it consumes a large amount of energy to grind chitin to nano size.[50] Alternatively, chemical modification is required to improve the efficiency of grinding. By pretreating chitin with sodium hydroxide, a partially deacetylated chitin nanowhisker can be obtained.[24] The partially deacetylated chitin nanowhiskers are

specifically deacetylated only on the surface and retain crystalline chitin inside. These manufacturing methods are top-down processes in which the higher-order structure of chitin is miniaturized to the crystallite unit by applying a mechanical load. As another method of producing nanochitin, there is a bottom-up production method in which chitin is dissolved and regenerated. Since the bottom-up method aggregates the dissolved chitin molecules to obtain a higher-order structure, an expensive crusher for applying a large load or chemical pretreatment is not required. In addition, there is a possibility that the shape of nanochitin can be controlled by examining the conditions of the regeneration process. Since chitosan is easily dissolved in an acidic aqueous solution, many particulate nanochitosans have been reported to be produced and used.[56] On the other hand, since chitin is difficult to dissolve in common solvent, there are few reports on the production of nanochitin by a bottom-up method. For example, Kadokawa et al. obtained nanochitin by dissolving chitin in an ionic liquid and then regenerating it.[57-59]

Alkaline chitin is a classic method of dissolving chitin.[60] When chitin is treated with sodium hydroxide, the hydroxy group of chitins is converted to sodium alkoxide. As a result, the hydrogen bonds constituting the chitin crystals are cleaved and dissolved in water as alkaline chitin. Alkaline chitin is used for chemical modification of chitin.[61] In addition, it can be easily regenerated into chitin by neutralization. Therefore, in this study, we try to manufacture nanochitin by a bottom-up approach. That is, nanochitin is produced by dissolving chitin as alkaline chitin and regenerating it.

3.2. Materials and methods

3.2.1. Materials

α-chitin powder from crab shell was purchased from Koyo Chemicals Industry Co., Ltd (chitin TC-L). The degree of deacetylation of chitin was 6%. Chitin nanofiber suspension was purchased from Marine Nano-fiber Co., Ltd. Analytical grade sodium hydroxide and acetic acid were purchased from Wako Pure Chemical Industries, Ltd. and used as received.

3.2.2. Preparation of chitin nanoparticles

The dissolution of chitin was made with some modifications with reference to previous research reports.[60] 3g of chitin was dispersed in 75 g of 45 wt% NaOH aqueous solution and stirred for 3 hours at room temperature, and then stirred under reduced pressure to remove air bubbles. After adding 222 g of ice to the dispersion, the mixture was stirred at 800 rpm for 20 hours with a magnetic stirrer at room temperature. To thus obtained alkaline chitin with 1 wt% concentration, an 11 wt% aqueous acetic acid solution was added dropwise under stirring to neutralize alkaline chitin. The regenerated chitin was collected by centrifugation and washed 4 times with distilled water. Distilled water was added to the regenerated chitin to a concentration of 1 wt%, and the mixture was vigorously stirred using mechanical homogenizer (T 25 ULTRA-TURRAX, IKA Japan) for 50 minutes.

3.2.3. Characterization of chitin nanoparticles

3.2.3.1. Morphological observation of chitin nanoparticle

Field emission scanning electron microscope (FE-SEM, JSM-6701F, JEOL, Japan) was used to observe the chitin nanoparticles. Chitin nanofibers were diluted by distilled water and dropped onto the surface of freshly cleaved mica substrate and dried overnight at 40 ^{o}C. The sample was coated with approximately 2 nm Pt layer by using an ion sputter coater and observed at 2.0 kV.

3.2.3.2. Measurement of nanoparticle size

Atomic force microscope (AFM, Nanocute, SII Instruments, Chiba, Japan) was also used to study surface morphology and measure size of chitin nanoparticles. The sample for observation was prepared by the same method as that of FE-SEM. To investigate the size distribution, 183 nanoparticles were randomly selected, and their diameters were measured.

3.2.3.3. Crystalline structure and crystallinity index determination

X-ray diffraction profile of the chitin nanoparticles was obtained in the range of 5^{o} to 40^{o} by using Ni-filtered CuKa from an X-ray generator (Ultima IV, Rigaku Corporation, Tokyo, Japan) operating at 40 kV and 30 mA. The dry chitin sample was prepared by freeze drying and pressing into flat sheet. The obtained profile was used to determine the crystallinity index (CI) by employing the equation: CI = (I_{110} - I_{am}) x 100/I_{110}, where I_{110} is maximum intensity of the 110 plane and I_{am} is the amorphous diffraction intensity at $16^{0}.^{30}$

3.2.3.4. Chemical structure determination

Infrared spectra of the samples were recorded with an FT-IR spectrophotometer (Spectrum 65, Perkin-Elmer Japan Co., Ltd. Yokohama, Japan) equipped with an attenuated total reflection (ATR) attachment with diamond/ZnSe crystal and recorded with a resolution of 4 cm^{-1} in the range of 600-4000 cm^{-1}.

3.2.3.5. Determination of thermal stability

Thermogravimetric (TG) analysis was run under nitrogen using Thermo Plus EVO II series (Rigaku Corporation, Japan). Sample mass was 5 mg, and a heating rate of 10 ^{o}C min^{-1} was used.

3.2.3.6. Light transmittance and viscosity measurement

UV-Vis spectrophotometer (V550; JASCO, Tokyo, Japan) was used to measure light transmittance of chitin nanoparticle dispersion in the range of 200 to 800 nm. For this measurement, chitin nanoparticle dispersion with 0.1 wt% was used.

Viscosity of chitin nanoparticle and commercially available chitin nanofiber suspension was measured by a Brookfield digital viscometer DV-E using spindle no. LV-2 (Brookfield Engineering Laboratories, Middleboro, MA, USA) at rotational speed of 20 rpm.

3.3. Results and discussion

3.3.1. Preparation of chitin nanoparticles

Ice was added to the chitin powder suspended in a 45% aqueous sodium hydroxide solution and the mixture was stirred at room temperature. Immediately it became a clear solution. This is because, the hydroxy groups (-OH) at the 3- and 6- positions of chitin are converted to sodium alkoxide (-ONa), thereby breaking the hydrogen bond between the chitin molecule. After stirring at room temperature for 20 hours, an aqueous acetic acid solution was added to the obtained aqueous alkaline chitin solution to neutralize sodium hydroxide. As the pH decreased, the transparent solution became cloudy. This is because the alkoxide returns to the hydroxy group, that is, the alkaline chitin is regenerated into chitin. The regenerated chitin interacts between the molecules and therefore aggregates. When this regenerated chitin was vigorously stirred with a homogenizer, the transparency of the suspension was improved. The ultraviolet-visible spectrum of this dispersion is shown in Figure 20. For example, the linear light transmittance at 600 nm was 71%. This indicates that the regenerated chitin is sufficiently small and dispersed well in water.[19] Substances that are sufficiently smaller than the wavelength of visible light (approximately 400 to 800 nm) become transparent because they are less likely to cause light scattering at the interface with water. The linear light transmittance of the dispersion was higher than that of chitin nanofibers produced by conventional mechanical grinding (23% at 600 nm). This suggests that the obtained regenerated chitin is smaller in size and easier to disperse than conventional chitin nanofibers, as will be described later.

A scanning electron microscope image of chitin in the dispersion is shown in Figure 21a. Fine particulate matter was observed. That is, chitin nanoparticles were obtained by a bottom-up process of dissolution, regeneration and pulverization of chitin with an alkali. Over a wide field of view, individual isolated uniform fine particles of about 10 nm could be observed. In order to investigate the size and the distribution of the nanoparticles, they were observed with an atomic force microscope (Figure 21b). Nanoparticles similar to the SEM image were observed. When the diameter was estimated from the height of the nanoparticles, all the particles were in the range of 2-11 nm, and the average particle diameter was 7 nm (Figure 21c). In addition, the size distribution was narrow because 5-9 nm particles accounted for 77% of the total. After adding ice to chitin soaked in alkali, it was stirred for 20 hours to prepare an aqueous solution of alkaline chitin. Sufficient stirring time was required to prepare small, uniform nanoparticles. When stirred for 3 or 10 hours, the particle size was large, and the distribution was wider. It is suggested that the entanglements of the alkaline chitin molecules are loosen and are completely dissolved by stirring over a long period of time.

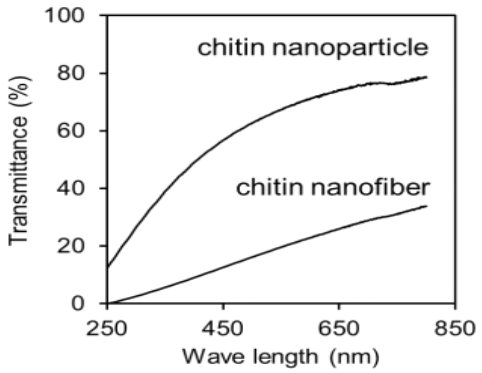

Figure 20. UV-Vis spectra of chitin nanoparticles and nanofibers.

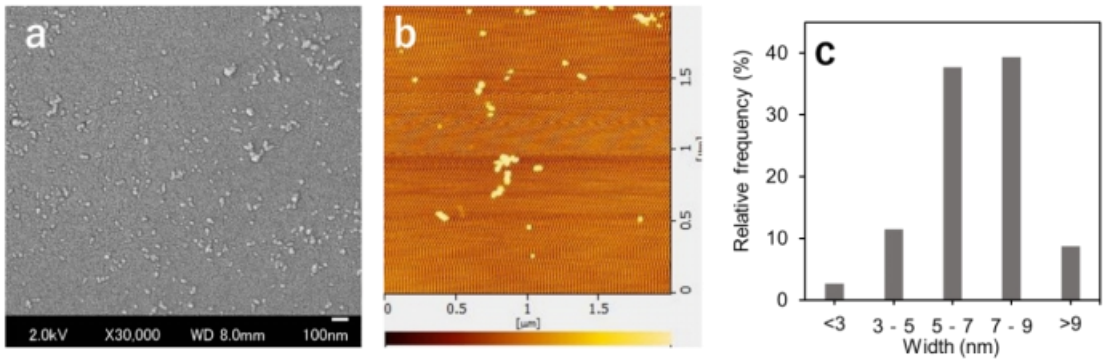

Figure 21. (a) SEM image, (b) AFM image and (c) size distribution of chitin nanoparticles.

3.3.2. Chemical structure of chitin nanoparticles

The degree of deacetylation of the chitin nanoparticles determined from the ratio of carbon and nitrogen atoms by elemental analysis was 6%, which was the nearly same value as the raw material chitin powder. That is, 45 wt% sodium hydroxide was used to dissolve chitin, but the deacetylation reaction did not occur since the treatment was performed at a temperature lower than room temperature. To evaluate the surface charge, the zeta potential of the nanoparticle was measured. It was +1.76 mV and had almost no charge in distilled water.

FT-IR spectra were measured to understand the structural changes in the production of chitin nanoparticles (Figure 22). The spectra of chitin nanoparticles and the original chitin powder were in good agreement. Peaks at OH stretching (3434 cm^{-1}), NH stretching (3257 cm^{-1} and 3103 cm^{-1}), CH bending and CH_3 symmetric deformation (1376 cm^{-1}), amide III (1308 cm^{-1}), and C-O-C asymmetric stretch in phase ring (1069 cm^{-1}), CO stretching (1009 cm^{-1}) of chitin molecules were confirmed.[33,62,63] The strong peak at 1553 cm^{-1} is derived

from the NH bend, CN stretch (amide II) of the acetamide group. The absorption intensity of the peak derived from the amido II of the regenerated chitin is in good agreement with that of the original chitin, indicating that the deacetylation reaction does not occur even after the sodium hydroxide treatment. On the other hand, the change of the peak derived from amide I is observed by the sodium hydroxide treatment. Two peaks at 1653 cm^{-1} and 1620 cm^{-1} in original chitin are changed to almost a single peak in regenerated chitin. This suggests a change in the crystal structure of chitin. That is, natural α-chitin consists of crystallites with extended chains and forms strong hydrogen bonds between molecules. The peak at 1653 cm^{-1} derives from the expansion and contraction of hydrogen bonds between the molecules of C=O and the NH group. The 1620 cm^{-1} band is then derived from hydrogen bonds in the sheet with C = O by both NH and CH_2OH. Thus, the change in the band of amide I suggests that the alkaline treatment disrupted the hydrogen bonds between the sheets of chitin crystals. Liu et al. Reported similar changes in the FT-IR spectrum by immersing chitin in 40 wt% sodium hydroxide for 4 hours.[64]

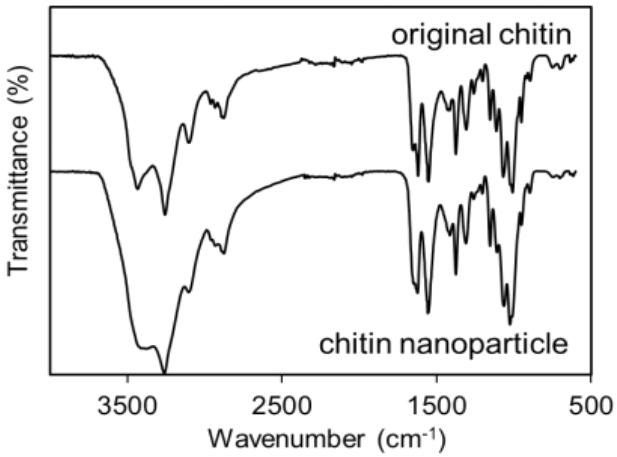

Figure 22. FT-IR spectra of (a) chitin nanoparticles and (b) original chitin.

3.3.3. Structure and formation mechanism of chitin nanoparticles

A wide-angle X-ray scattering measurement was used to investigate the crystal structure of chitin nanoparticles (Figure 23). The four peaks at 9.5°, 19.6°, 21.2°, and 23.5° correspond to the 020, 110, 120, and 130 planes of a typical α-type chitin crystal, respectively.[30] Therefore, the chitin nanoparticles obtained by regenerating chitin have the same type of chitin crystals as those derived from crustaceans. However, the relative crystallinity estimated from the comparison between the crystalline region and the amorphous region was 38.2% for chitin nanoparticles,[30] which was significantly lower than that of the original chitin (89.9%). This result suggests that the dissolved alkaline chitin is not completely regenerated into α-chitin crystals, and most of them have an amorphous structure. Previous studies have reported that the crystallinity is reduced from 51.9% to 29.3% by immersing chitin in 40 wt% sodium hydroxide for 4 hours at room temperature.[64]

Based on the above results, the formation mechanism of chitin nanoparticles is considered as follows. Natural chitin consists of microcrystals due to hydrogen bonds between chitin molecules. Hydroxy group (-OH) of chitin molecule is converted to sodium alkoxide(-ONa) by sodium hydroxide, breaking the intermolecular hydrogen bonds and collapsing the crystal structure, resulting in dissolution in water. The dissolved alkaline chitin is regenerated into chitin by neutralization. Regenerated chitin form aggregates due to inter- and intramolecular hydrogen bonds, dipole-dipole interactions, and London dispersion forces. The weak aggregates are easily separated and dispersed as nanoparticles by a shearing force exerted by vigorous stirring. As already described, in order to produce

chitin nanoparticles with narrow size distribution, stirring for 20 hours in the dissolution of chitin is important. The time is required to completely dissolve the chitin chain. Incomplete chitin dissolution will cause nanoparticles coarsening. Chitin nanoparticles obtained by such a bottom-up process may be able to control the shape of the particles depending on the regeneration conditions of alkaline chitin. This is a feature that cannot be achieved by the method of crushing the microcrystalline units of natural chitin by a top-down process.

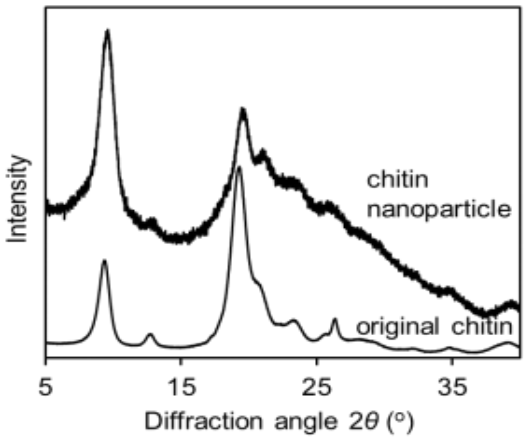

Figure 23. XRD profiles of (a) chitin nanoparticle and (b) original chitin.

3.3.4. Thermal properties of chitin nanoparticles

The thermal behavior of the chitin nanoparticles was evaluated using a thermogravimetric analyzer (Figure 24). There are three major thermogravimetric reductions for chitin nanoparticles. The initial weight loss began at about 55 ° C, which is associated with the evaporation of water. Chitin nanoparticles contain about 10% water, which is higher than the water content of the original chitin. This is because the chitin nanoparticles have a larger specific surface area and smaller crystallinity than the original

chitin, and therefore adsorbs more water molecules. Weight loss of the second chitin nanoparticles is observed in the range of about 220 °C to 375 °C, with maximum weight loss at 280 ° C. During that temperature change, the weight was reduced by 43.4%. It is speculated that this weight loss is due to the thermal decomposition of the functional groups of chitins, such as dehydration reaction, polymerization, and decomposition of amino and acetamide groups. The temperature range corresponding to the second weight loss of chitin nanoparticles was wider than that of the original chitin (250 - 350 °C). This suggests that the chitin nanoparticles have a larger surface area and more amorphous regions, which complicates the pyrolysis behavior. A third weight loss of chitin nanoparticles is observed in the range of about 450 °C to 650 °C, with the maximum weight loss peaking at 565 °C. The weight was reduced by 37% in that temperature range. According to differential thermal analysis, the exothermic peaks of chitin and its nanoparticles were 325 °C and 565 °C, respectively, which were significantly different. This major difference may be due to changes in the degradation process and mechanism associated with higher-order structural changes in chitin. That is, the chitin nanoparticles are obtained by regenerating in water. Therefore, hydrophilic part such as hydroxy group and some free amine groups of chitins are specifically distributed at the interface in contact with water, and such a structure contributes to the improvement of dispersibility in water. It is suggested that the specific distribution of hydrophilic functional groups on the surface affects not only the dispersibility in water but also the improvement of thermal behavior of the chitin nanoparticles.

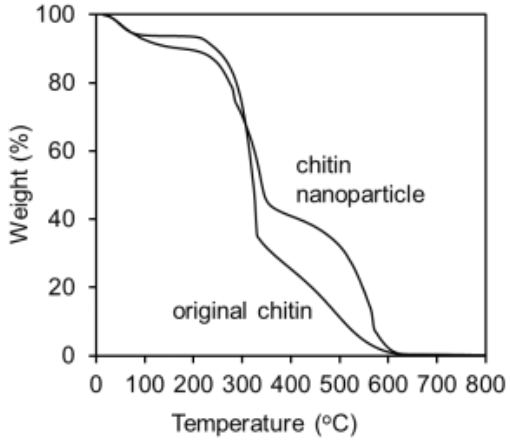

Figure 24. Pyrolysis behavior of chitin nanoparticle and original chitin.

3.3.5. Viscosity and dispersibility of chitin nanoparticles

The viscosity of aqueous dispersion of chitin nanoparticles was measured at different concentration and rotational speed of 20 rpm (Figure 25). Viscosity remained fair constant in the concentration range of 0.75 to 1.50%. On the other hand, the viscosity increased linearly from 1.75% depending on the concentration. This is because chitin nanoparticles approach and interact with each other in water as the concentration increases. That is, the critical concentration of chitin nanoparticles was 1.75%. The viscosity of the 1 wt% aqueous dispersion of chitin nanoparticle was 4.4 Pa.s at a rotation speed of 0.6 rpm. This value is very small compared to the viscosity of conventional chitin nanofiber (23.9 Pa.s). This is due to the difference in the shape of nanochitin. In addition, since chitin nanofibers are long, physical entanglement also occurs. Interactions between such fibers increase the viscosity of the dispersion. Therefore, in the production of chitin nanofibers, it is difficult to prepare the nanochitin at a high concentration, and it is usually processed at a low concentration of few percent. On the other hand, since the chitin nanoparticles have a low

viscosity, they can be produced at a relatively higher concentration. Increasing the concentration of nanochitin is important for reducing transportation costs.

The aqueous dispersion of chitin nanoparticles can be concentrated by centrifugation. The concentrated chitin nanoparticles can be uniformly dispersed again with a slight stirring. Its characteristics support the hydrophilicity of the surface of the regenerated chitin nanoparticles. On the other hand, in order to redisperse the chitin nanofibers aggregated by centrifugation, a strong mechanical treatment is required. This is because the concentrated nanofibers are intricately entwined with each other. Further, the surface of the nanofiber obtained by mechanical treatment has a hydrophilic surface and a hydrophobic surface, and the interaction between the hydrophobic surfaces works in water. On the other hand, the surface of the chitin nanoparticles regenerated in water is considered to be hydrophilic, which is considered to contribute to the improvement of redispersibility. The characteristics of chitin nanoparticles that can be concentrated and redispersed are advantageous in terms of reduction of transportation cost and ease of commercialization.

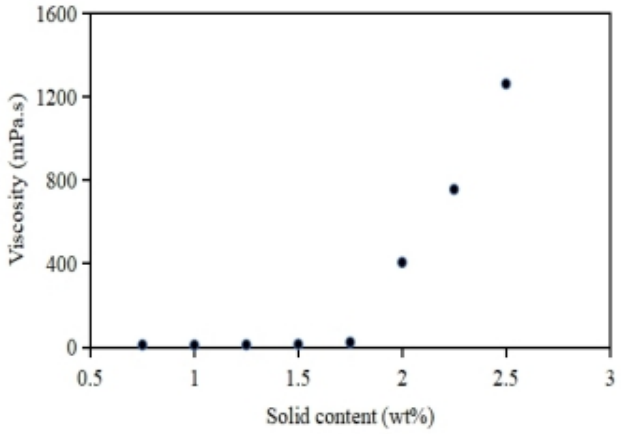

Figure 25. Viscosity of chitin nanoparticle at different solid content

3.4. Conclusion

Chitin nanoparticles were obtained by a bottom-up approach. First, chitin was treated with sodium hydroxide and dissolved as an alkaline salt. Then, the chitin solution was regenerated by neutralization and vigorously stirred to obtain chitin nanoparticles. Chitin nanoparticles have an average diameter of 7 nm and a narrow size distribution. Chitin nanoparticles have lower crystallinity and higher heat resistance than original chitin. This is because the higher-order structure of chitin is significantly changed by dissolving and regenerating. Moreover, since the surface is hydrophilic, individual particles are isolated and dispersed in water. Chitin nanoparticles have a lower viscosity and higher transparency than chitin nanofibers. This is because nanoparticles have less attractive force acting between substances and have less physical entanglement than chitin nanofibers. Since the viscosity is low, high concentration nanochitin can be produced. In addition, chitin nanoparticles can be easily concentrated by centrifugation and redispersed in water. These features are advantageous in reducing transportation costs, commercializing products, and evaluating functionality. It has been clarified that nanochitin has various physiological functions associated with its application to the skin and its administration. Chitin nanoparticles can be easily produced using only sodium hydroxide, which is inexpensive and can be used in foods. Therefore, chitin nanoparticles are expected to play an important role in industrial use as one of nanochitin.

Chapter 4

Preparation of partially deacetylated chitin nanoparticles by bottom-up approach.

4.1. Introduction

The chemical structure of chitin is similar to that of cellulose, which is the second most abundant biomass on earth after cellulose. However, its utilization is very small compared to cellulose. The main reason for the lack of utilization is that chitin is difficult to process because it dissolves only in special solvents. In recent years, nanochitin has been developed by applying nanocellulose manufacturing technology.[37] Since all naturally occurring chitins are aggregates of fibrous nanochitins[47,66] they can be pulverized to a nanometer scale after mechanical treatment.[15] Since nanochitin can be uniformly dispersed in water, it is easier to process than conventional chitin.[20,46] In addition, since it became easier to evaluate *in vitro* and *in vivo*, various physiological functions were clarified. For example, it has an effect on the skin,[11,13] an effect by taking it,[22,41] and an effect on plants.[42,43] Since improving moldability and discovering new functions are extremely important in promoting the use of chitin, further development of nanochitin manufacturing technology and exploration of potential functions are expected in the future. The method of refining macroscopic structures to nano-sized units by such crushing can be said to be a breakdown process. Since the process requires breaking the hydrogen bonds working between nanochitins, a crusher is needed to apply a strong mechanical load.[50] Therefore, there is a concern that the manufacturing cost will increase. Another approach to producing nanochitin is a bottom-up

process. It is a method of assembling chitin molecules and converting them into nano-sized higher-order structures. Since the process does not require a grinding operation, it has the potential to produce nanochitin in large quantities at low cost. In addition, it may be possible to control the morphology of nanochitin by studying the preparation conditions. Although there are few reports on the production of nanochitin by such a process,[57] we have recently succeeded in producing chitin nanoparticles by a bottom-up process.[67] Specifically, chitin is treated with a strong base, dissolved in water as alkaline chitin,[60,61,68] and then regenerated by a neutralization reaction to produce chitin nanoparticles with a diameter of 7 nm. Chitin nanoparticles are sometimes more advantageous in commercialization because they have higher dispersibility and lower viscosity than chitin nanofibers obtained by grinding because of their different shapes. Alkaline hydrolysis of chitin is widely used for obtaining chitosan. Partially deacetylated chitin nanofibers are related substances of chitin nanofibers.[24] The surface of the nanofiber is partially converted to an amino group by hydrolysis, and since it has a positive charge, it has excellent dispersibility. Since it also has the same functions as chitosan, products containing partially deacetylated nanochitin are on the market. If chitin nanoparticles can be partially deacetylated, it can be expected to expand their use as new nanochitin.

Therefore, in this study, we attempted to produce partially deacetylated chitin nanoparticles. That is, first, chitin is partially deacetylated as a pretreatment, and then it is dissolved in water as alkaline chitin, and then the aqueous solution is regenerated by neutralization to obtain nanochitin. A detailed evaluation was performed on the shape and physical properties of the regenerated chitin.

4.2. Materials and methods

4.2.1. Materials

Crab shell α-chitin powder was purchased from Koyo Chemicals Industry Co., Ltd (chitin TC-L). Sodium hydroxide and acetic acid with analytical grade were purchased from Wako Pure Chemical Industries, Ltd. and used as received.

4.2.2. Partial deacetylation of α-chitin

α-Chitin was partially deacetylated by refereeing to the previous report with slight modifications.[24] α-Chitin (9 g) was dispersed in 30 wt% (w/w) NaOH aqueous solution (300 g) and heated at a temperature of 90 ^{0}C for 4 hours while stirring continuously. The precipitate was collected and washed with distilled water till neutrality by repeated vacuum filtration. Portion of the collected precipitate was kept for determination of degree of deacetylation by elemental analysis. The rest of the sample was passed to the next nanoparticle synthesis process.

4.2.3. Preparation of partially deacetylated chitin nanoparticle

Alkaline chitin aqueous solution was prepared with slight modifications based on previous research report.[60,61,68] The partially deacetylated chitin was suspended in 45 wt% NaOH aqueous solution (150 g) and continuously stirred for 3 hours at room temperature and under reduced pressure to remove air bubbles. After 444 g ice was added, the mixture was stirred at 600 rpm for 16 hours at room temperature. Then, the resulting alkali chitin was neutralized with drop-wise addition of 11 wt% acetic acid under stirring at 800 rpm.

The regenerated chitin was collected as white cake and was washed at least 5 times by centrifuge. The pH was reduced to 3 by adding acetic acid before homogenization using Ika T25 basic S1 ultra-turrax for 5 minutes.

4.2.4. Preparation of partially deacetylated chitin nanoparticle cast film

15 mL of partially deacetylated chitin nanoparticle dispersion with 0.72 wt% (w/w) was mixed with 7 mL of acetone and stirred for 6 minutes. The resulting mixture was poured into the polyethylene sheet to dry at 35 ^{0}C for 24 hours.

4.2.5. Characterization of partially deacetylated chitin nanoparticle

4.2.5.1. Morphological observation

Field emission scanning electron microscope (FE-SEM, JSM-6701F, JEOL, Japan) was used to observe the surface morphology of the partially deacetylated α-chitin nanoparticles and cast film. Diluted sample was dropped on the surface of freshly cleaved mica substrate, dried at 35 ^{0}C, and coated with an approximately 2 nm Pt layer by using an ion sputter coater and observed at 2.0 kV. Similarly, the cast film was also coated with Pt by an ion sputter to observe the surface morphology.

4.2.5.2. Measurement of the size

Atomic force microscope (AFM, Nanocute, SII Instruments, Japan) was used to observe the surface morphology and measure width of partially deacetylated chitin nanoparticle.

Diluted suspension was dropped on the freshly cleaved mica substrate, dried at 35 ^{0}C, and surface characteristics was observed. To investigate the size distribution, 126 nanoparticles were randomly selected, and their diameters were measured.

4.2.5.3. Crystalline structure and crystallinity index determination

Crystallinity of partially deacetylated chitin nanoparticle in the range of 5^0 to 45^0 was studied by using Ni-filtered CuKα from an X-ray diffractometer (Ultima IV, Rigaku Corporation, Japan) operating at 40 kV and 40 mA. The suspension was freeze dried and pressed into flat sheet to obtain the XRD profile. This diffraction profile was used to calculate the relative crystallinity index using CI = (I_{110} - I_{am}) x 100/I_{110}, where I_{110} is the maximum intensity of the 110 plane and I_{am} is the amorphous diffraction intensity at 16^0.[30]

4.2.5.4. Determination of chemical structure

Infrared spectra of partially deacetylated chitin nanoparticle in the range of 4000 - 600 cm^{-1} was recorded using FT-IR spectrophotometer (Spectrum 65, Perkin-Elmer Japan, Japan) equipped with an attenuated total reflection (ATR) attachment with diamond/ZnSe crystal with a resolution of 4 cm^{-1}.

4.2.5.5. Light transmittance and zeta potential

UV-Vis spectrophotometer (UV-2600i, Shimadzu Corporation, Japan) was used to measure regular light transmittance of partially deacetylated chitin nanoparticle dispersion

and the cast film, respectively. The dispersion sample was diluted to 0.1 wt% for the measurement.

Zeta potential of partially deacetylated chitin nanoparticle was determined using zeta potential and particle size analyzer (ELSZ-1000, Otsuka Electronics Co., Ltd.). The concentration of the sample for this measurement was 0.008 wt%.

4.2.5.6. Thermal analysis

Thermogravimetric (TG) data was recorded using thermogravimetric analyzer (Thermo Plus EVO II series, Rigaku, Japan) under nitrogen atmosphere with a heating rate of 10 ^{0}C min^{-1}. The sample was prepared by drying the suspension at 40 ^{0}C and crashing into smaller size. About 5 mg of the sample was subjected to the analysis.

4.3. Results and discussion

4.3.1. Self-assembly, morphology, and transparency of partially deacetylated chitin nanoparticle

The deacetylation of α-chitin, which was conducted by treating with 30 wt% NaOH aqueous solution at temperature of 90 ^{0}C for 4 hours, was able to raise the degree of deacetylation from the original value of 6% to 27%, as determined from the elemental analysis. The result is in good agreement with the results reported in the past.[24]

The partially deacetylated α-chitin was treated with 45% aqueous NaOH solution at room temperature, and then ice was added to dissolve it. It was a viscous, clear aqueous solution.

This is because the hydroxy groups of chitin molecule are converted to the sodium alkoxide, which breaks the hydrogen bond interacting between the molecules. The α-type crystal structure of chitin breaks and dissolves in water easily as alkaline chitin. The dissolved alkaline chitin solution was neutralized with an acetic acid aqueous solution. By neutralization, the sodium alkoxide of alkaline chitin is regenerated into hydroxy groups, becoming insoluble in water, and forming aggregates. The degree of deacetylation of regenerated chitin nanoparticle was found to be 28%. Thus, the alkaline treatment was not affected the degree of deacetylation since the increase was only 1%. Figure 26a and b shows the SEM and AFM images of the regenerated chitin, respectively. The regenerated partially deacetylated chitin was in the form of fine particles. Uniform nano-sized particles were observed throughout the field of view in each microscopic image. This suggests that the dissolved chitin interacted with each other by neutralization to form nanoparticles. When over 100 nanoparticles were randomly selected and the nanoparticles diameter was estimated from the height direction of the AFM images, it was in the range of 2.12-7.62 nm (Figure 26c). The average size was found to be 4 nm. The average particle size of the non-deacetylated chitin nanoparticles was 7 nm, so the nanoparticles prepared in this study were smaller.[67] This difference in size is due to the difference in chemical structure. Since a part of the chitin molecule was converted into an amino group in the partially deacetylated chitin, the interaction between the molecules is weaker than that of the unreacted chitin. Therefore, it is considered that the particles were regenerated as smaller particles by neutralization.

Partially deacetylated chitin nanoparticles homogeneously dispersed in water and was optically transparent (Figure 27a). UV-Vis spectrum of the dispersion with 0.1% concentration was show in Figure 27b. The linear transmittance of the dispersion was over 80% at the wavelength of visible light. For example, the permeability at 600 nm was 87%, which was higher than that of non-deacetylated chitin nanoparticles (71%).[67] The improvement in dispersibility is due to the pretreatment of chitin for deacetylation. Twenty eight percent of the acetylglucosamine units of chitin are deacetylated. Since the amino group ($-NH_2$) generated by the hydrolysis reaction is converted to acetate ($-NH_3^+$ CH_3COO^-) by neutralization, the affinity for water is improved. In addition, the positive charge on the surface causes electrostatic repulsion and improves dispersibility. In fact, the zeta potential of the nanoparticles at pH 3 was +12.84 mV. From the above, the deacetylation treatment enables control of the size of nanoparticles and improvement of dispersibility in water.

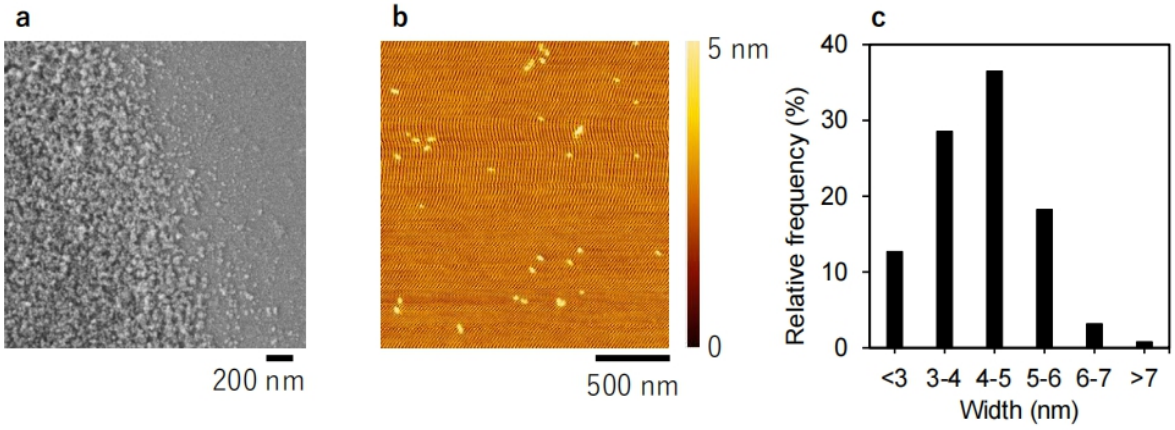

Figure 26. (a) SEM, (b) AFM images of partially deacetylated chitin nanoparticles, and (c) the size distribution estimated from AFM image.

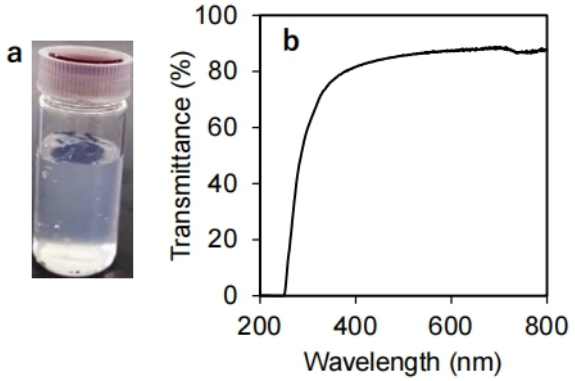

Figure 27. (a) Appearance and (b) UV-Vis spectrum of partially deacetylated chitin nanoparticle water dispersion.

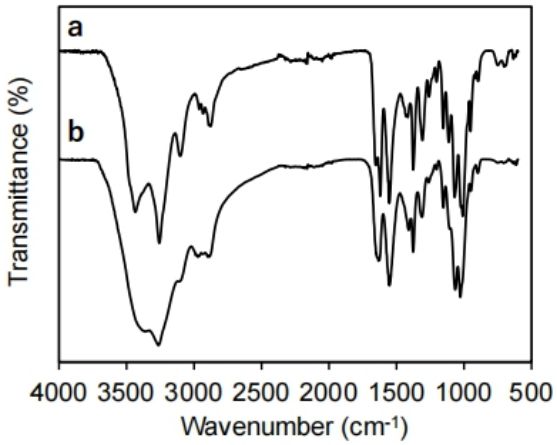

Figure 28. FTIR spectra of (a) original chitin and (b) partially deacetylated chitin nanoparticle.

4.3.2. Chemical, crystalline, and thermal properties of the partially deacetylated α-chitin nanoparticle

The FT-IR spectra of original chitin and partially deacetylated chitin nanoparticles are shown in Figure 28. In the spectrum of the original chitin, OH stretch band at 3434 cm^{-1}, NH stretching band at 3257 cm^{-1}, amide band I at 1653 and 1620 cm^{-1}, and amide II band at

1559 cm^{-1} are observed. On the other hand, in the spectrum of nanoparticles, the peak derived from the acetamide group becomes relatively smaller with deacetylation. Moreover, the amide I peaks of α-chitin divided into 1653 and 1620 cm^{-1} changed to single peak observed at around 1635 cm^{-1}. This suggests a change in the crystal structure of α-chitin.[64] That is, natural chitin forms strong hydrogen bonds between molecules. The peak at 1653 cm^{-1} derives from hydrogen bonds between the molecules of C=O and the NH group. The 1620 cm^{-1} band is derived from hydrogen bonds in the sheet with C=O by both NH and CH_2OH. Thus, the change in the band of amide I suggests that the alkaline treatment disrupted the hydrogen bonds of chitin crystals.

Figure 29 shows the X-ray diffraction patterns of the original chitin and nanoparticles. In the diffraction pattern of the original chitin, the peaks at 9.5^0, 19.5^0, 20.9^0, and 23.4^0 correspond to 020, 110, 120 and 130 planes of α-chitin crystal, respectively.[30] On the other hand, in nanoparticles, their peak intensities are significantly reduced. The relative crystallinity estimated from the ratio of the intensities of the crystalline and amorphous regions decreased from 90.0% to 38.0%. This value suggests that the partially deacetylated chitin nanoparticles is dominated by the amorphous region and is close to that of non-deacetylated chitin nanoparticles (38.2%). It is a feature of the nanoparticles obtained by regeneration of the chitin solution.[67]

Figure 30 shows the results of thermogravimetric analysis of the original chitin and deacetylated chitin nanoparticles. The thermogravimetric curve of chitin nanoparticles mainly consists of three weight reductions. The initial weight loss occurs in the range from

room temperature to about 125 ^{0}C, which is associated with evaporation of water. The amount of water contained in the nanoparticles is higher than that of the original chitin. This is due to the fact that the nanoparticles have a large specific surface area and consist of amorphous regions. Second loss is observed in the range of about 200 ^{0}C to 370 ^{0}C, with the maximum weight loss at 355 ^{0}C. The weight loss is due to the thermal decomposition of the functional groups of chitins, such as dehydration reaction, polymerization and decomposition of amino and acetamide groups. The residual weight of the nanoparticles at 370 ^{0}C was 40%, which is higher than that of the original chitin (29%) indicating improvement of the thermal stability. The third weight loss is observed in the range of 370 ^{0}C to 600 ^{0}C, with the maximum weight loss at 510 ^{0}C, which is very different from that of the original chitin. The difference may be associated with structural change in chitin. Partially deacetylated chitin with amorphous structure may influence the thermal behavior.

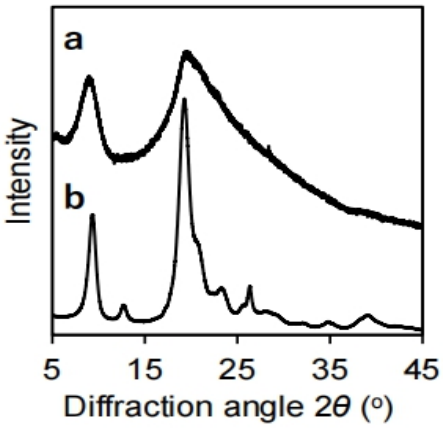

Figure 29. X-ray diffraction profile of (a) partially deacetylated chitin nanoparticle and (b) original chitin.

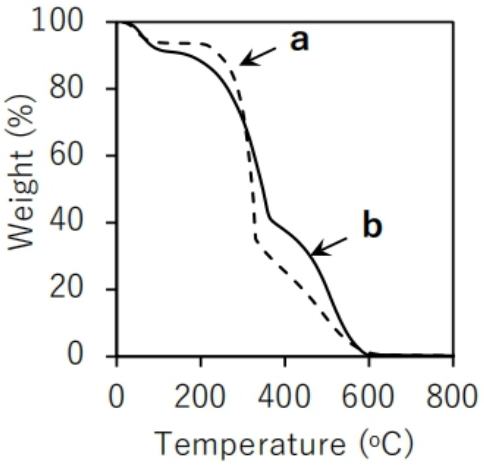

Figure 30. TGA curve of (a) original chitin and (b) partially deacetylated chitin nanoparticle.

4.3.3. Surface morphology and transparency of partially deacetylated α-chitin nanoparticle film

Since the partially deacetylated chitin nanoparticles are clearly dispersed in water, they can be easily converted into a thin film by being applied to the surface of the substrate. The cast film was optically transparent. Figure 31a shows the SEM image of the surface of the nanoparticle thin film. The thin film consists of densely aggregated uniform nanoparticles and a smooth surface. Figure 31b shows the UV-Vis spectrum of the transparent film with a thickness of 14.2 μm. The linear transmittance of the film in the visible light region was 83% or more. The high transparency may be due to the following three reasons suppressed the light scattering for the film. That is, 1. the surface of the film is smooth, 2. the nanoparticles are densely packed and there are no air voids in the film, and 3. the film is composed of amorphous nanoparticles.[69]

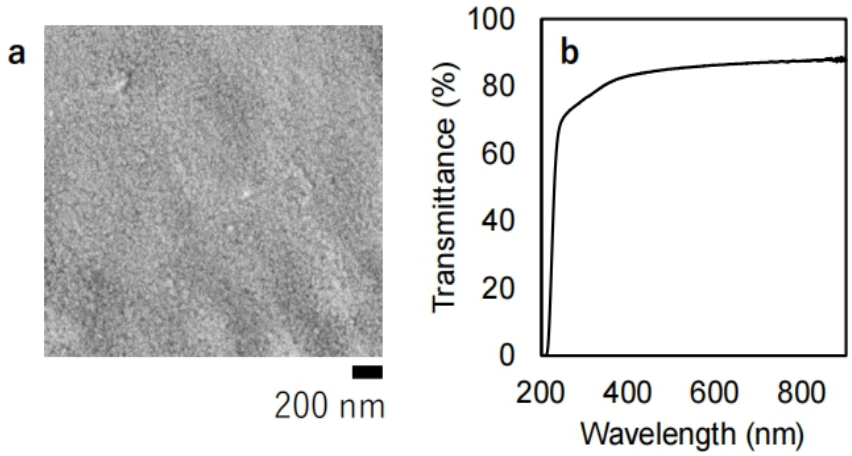

Figure 31. (a) SEM image and (b) UV-vis spectrum of partially deacetylated chitin nanoparticle thin film.

4.4. Conclusion

Partially deacetylated chitin nanoparticles were produced by a bottom-up approach. That is, it was obtained by dissolving partially deacetylated chitin as alkaline chitin and regenerating it by neutralization. Due to smaller size, surface properties, and amorphous structure, the nanoparticles have higher dispersibility and higher heat resistance than conventional chitin. In addition, it can be easily converted into a transparent film by the casting method. The nanochitin obtained by the bottom-up process uses food-grade chemicals and does not require a special crusher. Therefore, the use of the new nanochitin will be clarified by examining its function and characteristics in detail in the future.

General summary

Chitin is one of the most abundant polysaccharides in nature. The chemical structure is very close to the structure of cellulose. The only difference is the hydroxy group that exists at C-2 position is substituted by acetamide group in the case of chitin. Chitin based products are characterized to be biodegradable and biocompatible. Now a days industries that produces nanochitin and use it as raw material is increasing. Different functional and biomaterials is being produced from nanochitin. Various research are being carried out to apply nanochitin in renewable energy generation, wound healing, skin care products, tissue engineering, drug delivery etc. Conventionally nanochitin is being produced by break down approach. This approach requires strong impact generating equipment such as ultrafine grinder. To increase the feasibility of nanochitin containing products and diversify the application, alternative production method with variation of dispersion property needs to be investigated. As another method of nanochitin production, bottom-up approach is considered as novel method. This alternative method produces nanochitin with property differs from the convention method.

This study investigated the production of nanochitin by break down and bottom-up method. The obtained nanochitins size, morphonology, crystallinity, chemical structure, dispersion property, and transparency was characterized in detail.

In chapter 1, nanofibrillation of partially deacetylated chitin using low power ultrasonic machine was explained. This machine can be purchased inexpensively and is commonly used to wash glassware. Chitin was disintegrated into nanofiber with the support of

electrostatic repulsion that emanates from cationized amino group on the surface of chitin. The optimum nanofibrillating frequency and ultrasonication time was determined by comparing yield, morphology, and dispersion properties. The optimized variables, ultrasonication frequency and time, was significantly affected the yield, size, and dispersion property. The ultrasonication process, in general the mechanical treatment, consumes less energy and is contamination-free. The result of this study promotes the use of partially deacetylated chitin nanofiber in pharmaceuticals and medical devices.

In chapter 2, individualization of natural chitin using ball milling machine under neutral condition was described. Nanofibrillating efficiency of milling ball size, weight, and time was optimized using the dispersion property and dried film characteristics. Ball weight was reduced the size and crystallinity of chitin nanofiber compared to the other parameters. The relationship between milling variables and characteristics of the dispersion was explained in detail. This study adds value to the effort of producing nanofiber from non-modified chitin and understanding the characteristics of break down process. Moreover, the employed method can be characterized by cheap operational cost and simple process. This makes ball milling a candidate for the industrial production of chitin nanofiber.

In chapter 3, bottom-up method of producing nanochitin was described. Instead of using powerful machine, chemical was used to prepare nanochitin. Concentrated NaOH and ice was completely disentangled the chitin chain, which then aggregated by acetic acid. The obtained nanochitin was characterized to have a dominant amorphous region, uniform size distribution, and better thermal stability. The size is extremely smaller than the nanochitin

prepared using break down method. Dispersibility in water and easiness of separability makes the product a choice for the industrial production. Its low viscosity also supports the exportation of this product at high concentration. In general, the preparation method was cheaper, and the procedure is simpler than the break down method. It can better fit to industrial production needed characteristics.

In chapter 4, the preparation of partially deacetylated nanochitin using bottom-up approach was explained. The method employed in this part had some similarity with chapter 3, except imparting partial deacetylation stage. The obtained nanochitin was smaller than the non-deacetylated nanochitin. Because of the electrostatic repulsion of the cationized amino group on the surface of nanochitin better dispersibility and transparency was registered. Like non-deacetylated chitin the crystallinity index was lower than the pure chitin. The method employed to prepare partially deacetylated chitin nanoparticle was cheaper and easier at industrial level compared to the conventional procedure. However, the uses and applications need to be clarified.

References

1. Nair, K.G.; Dufresne, A. Crab shell whisker reinforced natural rubber nanocomposites. Processing and swelling behavior. *Biomacromolecules* **2003**, 4, 657–665.

2. Agboh, O. C.; Qin, Y. Chitin and chitosan fibers. *Polymers for Advanced Technologies* **1997**, 8(6), 355–365.

3. Rudall, K. M. The Chitin/Protein Complexes of Insect Cuticles. *Advances in Insect Physiology* **1963**, 1(C), 257–313.

4. Minke, R.; Blackwell, J. The structure of α-chitin. *Journal of Molecular Biology* **1978**, 120(2), 167–181.

5. Fang, Y.; Duan, B.; Lu, A.; Liu, M.; Liu, H.; Xu, X.; Zhang, L. Intermolecular Interaction and the Extended Wormlike Chain Conformation of Chitin in NaOH/Urea Aqueous Solution. *Biomacromolecules* **2015**, 16(4), 1410–1417.

6. Chen, B.; Sun, K.; Zhang, K. Rheological properties of chitin/lithium chloride, N, N-dimethyl acetamide solutions. *Carbohydrate Polymers* **2004**, 58(1), 65–69.

7. Hu, X.; Du, Y.; Tang, Y.; Wang, Q.; Feng, T.; Yang, J.; Kennedy, J. F. Solubility and property of chitin in NaOH/urea aqueous solution. *Carbohydrate Polymers* **2007**, 70(4), 451–458.

8. Feng, F.; Liu, Y.; Hu, K. Influence of alkali-freezing treatment on the solid state structure of chitin. *Carbohydrate Research* **2004**, 339(13), 2321–2324.

9. Einbu, A.; Naess, S. N.; Elgsaeter, A.; Vårum, K. M. Solution properties of chitin in alkali. *Biomacromolecules* **2004**, 5(5), 2048–2054.

10. Kadokawa, J. I.; Takegawa, A.; Mine, S.; Prasad, K. Preparation of chitin nanowhiskers using an ionic liquid and their composite materials with poly(vinyl alcohol). *Carbohydrate Polymers* **2011**, 84(4), 1408–1412.

11. Izumi, R.; Komada, S.; Ochib, K.; Karasawa, L.; Osaki, T.; Murahata, Y.; Tsuka, T.; Imagawa, T.; Itoh, N.; Okamoto, Y.; et al. Favorable effects of superficially deacetylated chitin nanofibrils on the wound healing process. *Carbohydrate Polymers* **2015**, 123, 461–467.

12. Izumi, R.; Azuma, K.; Izawa, H.; Morimoto, M.; Nagashima, M.; Osaki, T.; Tsuka, T.; Imagawa, T.; Ito, N.; Okamoto, Y.; et al. Chitin nanofibrils suppress skin inflammation in atopicdermatitis-like skin lesions in NC/Nga mice. *Carbohydrate Polymers* **2016**, 146, 320–327.

13. Azuma, K.; Koizumi, R.; Izawa, H.; Morimoto, M.; Saimoto, H.; Osaki, T.; Yamashita, M.; Tsuka, T.; Imagawa, T.; Okamoto, Y.; et al. Hair growth-promoting activities of chitosan and surface-deacetylated chitin nanofibers. *International Journal of Biological Macromolecule* **2019**, 126, 11–17.

14. Azuma, K.; Osaki, T.; Wakuda, T.; Ifuku, S.; Saimoto, H.; Tsuka, T.; Imagawa, T.; Okamoto, Y.; Minami, S. Beneficial and preventive effect of chitin nanofibrils in a

dextran sulfate sodium-induced acute ulcerative colitis model. *Carbohydrate Polymers* **2012**, 87, 1399–1403.

15. Ifuku, S.; Nogi, M.; Abe, K.; Yoshioka, M.; Morimoto, M.; Saimoto, H.; Yano, H. Preparation of chitin nanofibers with a uniform width as α-chitin from crab shells. *Biomacromolecules* **2009**, 10, 1584–1588.

16. Chen, P.Y.; Lin, Y.M.; McKittrick, J.; Meyers, M.A. Structure and mechanical properties of crab exoskeletons. *Acta Biomaterialia* **2008**, 4, 587–596.

17. Ifuku, S.; Nogi,. M.; Abe, K.; Yoshioka, M.; Morimoto, M.; Saimoto, H.; Yano, H. Simple preparation method of chitin nanofibers with a uniform width of 10–20nm from prawn shell under neutral conditions. *Carbohydrate Polymers* **2011**, 84, 762–764.

18. Ifuku, S.; Nomura, R.; Morimoto, M.; Saimoto, H. Preparation of Chitin Nanofibers from Mushrooms. *Materials* **2011**, 4, 1417–1425.

19. Ifuku, S.; Morooka, S.; Nakagaito, A.N.; Morimoto, M.; Saimoto, H. Preparation and characterization of optically transparent chitin nanofiber/(meth)acrylic resin composites. *Green Chemistry* **2011**, 13, 1708–1711.

20. Torres-Rendon, J.G.; Femmer, T.; Laporte, L.; Tigges, T.; Rahimi, K.; Gremse, F.; Zafarnia, S.; Lederle, W.; Ifuku, S.; Wessling, M.; et al. Bioactive gyroid scaffolds formed by sacrificial templating of nanocellulose and nanochitin hydrogels as

instructive platforms for biomimetic tissue engineering. *Advanced Materials* **2015**, 27, 2989–2995.

21. Torres-Rendon, J.G.; Schacher, F.H.; Ifuku, S.; Walther, A. Mechanical performance of macrofibers of cellulose and chitin nanofibrils aligned by wet-stretching: A critical comparison. *Biomacromolecules* **2014**, 15, 2709–2717.

22. Goto, M.; Iohara, D.; Michihara, A.; Ifuku, S.; Azuma, K.; Kadowaki, D.; Maruyama, T.; Otagiri, M.; Hirayama, F.; Anraku, M. Effects of surface-deacetylated chitin nanofibers on non-alcoholic steatohepatitis model rats and their gut microbiota. *International Journal of Biological macromolecule* **2020**, 164, 659–666.

23. Ifuku, S.; Yamada, K.; Morimoto, M.; Saimoto, H. Nanofibrillation of dry chitin powder by starburst system. *Journal of nanomaterials* **2012**, 645624.

24. Fan, Y.; Saito, T.; Isogai, A. Individual chitin nano-whiskers prepared from partially deacetylated α-chitin by fibril surface cationization. *Carbohydrate Polymers* **2010**, 79, 1046–1051.

25. Bang, J.H.; Suslick, K.S. Applications of ultrasound to the synthesis of nanostructured materials. *Advanced Materials* **2010**, 22, 1039–1059.

26. Ambedkar, B.; Nagarajan, R.; Jayanti, S. Investigation of high-frequency, high-intensity ultrasonics for size reduction and washing of coal in aqueous medium. *Industrial and Engineering Chemistry Research* **2011**, 50, 13210–13219.

27. McQueen, D.H. Frequency dependence of ultrasonic cleaning. *Ultrasonics* **1986**, 24, 273–280.

28. Yamaguchi, T.; Nomura, M.; Matsuoka, T.; Koda, S. Effects of frequency and power of ultrasound on the size reduction of liposome. *Chemistry and physics of lipids* **2009**, 160, 58–62.

29. Lu, Y.; Sun, Q.; She, X.; Xia, Y.; Liu, Y.; Li, J.; Yang, D. Fabrication and characterisation of α-chitin nanofibers and highly transparent chitin films by pulsed ultrasonication. *Carbohydrate Polymers* **2013**, 98, 1497–1504.

30. Zhang, Y.; Xue, C.; Xue, Y.; Gao, R.; Zhang, X. Determination of the degree of deacetylation of chitin and chitosan by X-ray powder diffraction. *Carbohydrate Research* **2005**, 340, 1914–1917.

31. Brotchie, A.; Grieser, F.; Ashokkumar, M. Effect of power and frequency on bubble-size distributions in acoustic cavitation. *Physical review letters* **2009**, 102, 084302.

32. Koda, S.; Kimura, T.; Kondo, T.; Mitome, H. A standard method to calibrate sonochemical efficiency of an individual reaction system. *Ultrasonics Sonochemistry* **2003**, 10, 149–156.

33. Pereira, A.G.B.; Muniz, E.C.; Hsieh, Y.L. Chitosan-sheath and chitin-core nanowhiskers. *Carbohydrate Polymers* **2014**, 107, 158–166.

34. Goodrich, J.D.; Winter, W.T. α-Chitin nanocrystals prepared from shrimp shells and their specific surface area measurement. *Biomacromolecules* **2007**, 8, 252–257.

35. Derjaguin, B.; Landau, L. Theory of the stability of strongly charged lyophobic sols and of the adhesion of strongly charged particles in solutions of electrolytes. *Progress in Surface Science* **1993**, 43, 30–59.

36. Verwey, E.J.W. Theory of the stability of lyophobic colloids. *Journal of Physical and Colloid Chemistry* **1947**, 51, 631–636.

37. Abe, K.; Iwamoto, S.; Yano, H. Obtaining cellulose nanofifibres with a uniform width of 15 nm from wood. *Biomacromolecule* **2007,** 8, 3276-3278.

38. Das, P; Heuser, T.; Wolf, A.; Zhu, B.; Demco, D. E.; Ifuku, S.; Walther, A. Tough and catalytically active hybrid biofibers wet-spun from nanochitin hydrogels. *Biomacromolecules* **2012**, 13, 4205−4212.

39. Ifuku S.; Nogi M.; Yoshioka M.; Morimoto M.; Yano H.; Saimoto H. Fibrillation of dried chitin into 10–20 nm nanofibers by a simple grinding method under acidic conditions. *Carbohydrate Polymers* **2010**, 81, 134-139.

40. Tan A.; Zhou X.; Wu K.; Yang D.; Jiao Y.; Zhou C. Tannic acid/Ca^{II} anchored on the surface of chitin nanofiber sponge by layer-by-layer deposition: Integrating effective antibacterial and hemostatic performance. *International Journal of Biological Macromolecules* **2020**, 159, 304-315.

41. Anraku, M.; Tabuchi, R.; Ifuku, S.; Nagae, T.; Iohara, D.; Tomida, H.; Uekama, K.; Maruyama, T.; Miyamura, S.; Hirayama, F.; Otagiri, M. An oral absorbent, surface-deacetylated chitin nano-fiber amelioratesrenal injury and oxidative stress in 5/6 nephrectomized rats. *Carbohydrate Polymers* **2017**, 161, 21–25.

42. Egusa, M.; Matsui, H.; Urakami, T.; Okuda, S.; Ifuku, S.; Nakagami, H.; Kaminaka, H. Chitin nanofiber elucidates the elicitor activity of polymeric chitin in plants. *Frontiers in Plant Science* **2015**, 6, 1098.

43. Parada, R. Y.; Egusa, M.; Aklog, Y. F.; Miura, C.; Ifuku, S.; Kaminaka, H. Optimization of nanofibrillation degree of chitin for induction of plant disease resistance: Elicitor activity and systemic resistance induced by chitin nanofiber in cabbage and strawberry. *International Journal of Biological Macromolecules* **2018**, 118, 2185–2192.

44. Vincent J.; Wegst U.; Design and mechanical properties of insect cuticle. *Arthropod Structure & Development*, **2004**, 33, 187-199.

45. Wada M.; Saito Y.; Lateral thermal expansion of chitin crystals. *Journal of Polymer Science, Part B: Polymer Physics* **2001**, *39*, 168-174.

46. Ifuku, S.; Ikuta, A.; Egusa, M.; Kaminaka, H.; Izawa, H.; Morimoto, M.; Saimoto, H. Preparation of high-strength transparent chitosan film reinforced with surface-deacetylated chitin nanofibers. *Carbohydrate Polymers* **2013**, 98(1), 1198–1202.

47. Raabe, D.; Romano, P.; Sachs, C.; Fabritius, H.; Al-Sawalmih, A.; Yi, S.-B.; Servos, G.; Hartwig, H.G. Microstructure and crystallographic texture of the chitin–protein network in the biological composite material of the exoskeleton of the lobster Homarus americanus. *Material Science and Engineering A* **2006**, 421, 143–153.

48. Ifuku S.; Morooka S.; Morimoto M.; Saimoto H. Acetylation of chitin nanofibers and their transparent nanocomposite films. *Biomacromolecule* **2010**, *11*, 1326-1330.

49. Shams M.I.; Ifuku S.; Nogi M.; Oku T.; Yano H. Fabrication of optically transparent chitin nanocomposites. *Applied Physics A* **2011**, 102, 325–331.

50. Dutta, A. K.; Yamada, K.; Izawa, H.; Morimoto, M.; Saimoto, H.; Ifuku, S. Preparation of chitin nanofibers from dry chitin powder by star burst system: dependence on number of passes. *Journal of Chitin and Chitosan Science* **2013,** 1, 59–64.

51. Liu L.; Chenhuang J.; Lu Y.; Fan Y.; Wang Z. Facile preparation of nanochitins via acid assisted colloid milling in glycerol. *Cellulose* **2020**, *27*, 6935–6944.

52. Tran T.H.; Nguyen H.; Hao L.T.; Kong H.; Park J.M.; Jung S.; Cha H.G.; Lee J.Y.; Kim H.; Hwan S.Y.; Park J.; Oh D.X. A ball milling-based one-step transformation of chitin biomass to organo-dispersible strong nanofibers passing highly time and energy consuming processes. *International Journal of Biological Macromolecule* **2019**, 125, 660-667.

53. Zhong T.; Wolcott M.P.; Liu H.; Glandon N.; Wang J. The influence of pre-fibrillation via planetary ball milling on the extraction and properties of chitin nanofibers. *Cellulose* **2020**, 27, 6205-6216.

54. Shin, H.; Lee, S.; Suk Jung, H.; Kim, J. B. Effect of ball size and powder loading on the milling efficiency of a laboratory-scale wet ball mill. *Ceramics International* **2013**, 39(8), 8963–8968.

55. Fan, Y.; Saito, T.; Isogai, A. Preparation of chitin nanofibers from squid pen *b*-Chitin by simple mechanical treatment under acid conditions. *Biomacromolecules* **2008**, 9, 1919–1923.

56. Elsabee, M. Z.; Naguib, H. F.; Morsi, R. E. Chitosan based nanofibers. review, *Material Science and Engineering C* **2012,** 32, 1711-1726.

57. Tajiri, R.; Setoguchi, T.; Wakizono, S.; Yamamoto, K.; Kadokawa, J. Preparation of self-assembled chitin nanofibers by regeneration from ion gels using calcium halide·dihydrate/methanol solutions. *Journal of Biobased Material and Bioenergy* **2013**, 7, 655-659.

58. Salaberria, A.M.; Labidi, J; Fernandes, S.C.M. Different routes to turn chitin into stunning nano-objects. *European Polymer Journal* **2015**, 68, 503–515.

59. Zhong, C; Cooper, A; Kapetanovic, A; Fang, Z; Zhang, M.; Rolandi, M. A facile bottom-up route to self-assembled biogenic chitin nanofibers. *Soft Matter* **2010**, 6, 5298–5301.

60. Tokura, S.; Nishi, N.; Tsutsumi, A.; Somorin, O. Studies on chitin VIII. Some properties of water soluble chitin derivatives. *Polymer Journal* **1983**, 15, 485-489.

61. Tokura, S.; Nishimura, S.; Nishi N. Studies on chitin IX. Specific binding of calcium ions by carboxymethyl-chitin. *Polymer Journal* **1983**, 15, 597-602.

62. Soetemans, L.; Uyttebroek, M.; Bastiaens, L. Characteristics of chitin extracted from black soldier fly in different life stages. *International Journal of Biological Macromolecule* **2020,** 165, 3206-3214.

63. Gbenebor, O.P.; Adeosun, S.O.; Lawal, G.I.; Jun, S.; Olaleye, S.A. Acetylation, crystalline and morphological properties of structural polysaccharide from shrimp exoskeleton. *Engineering Science and Technology, an International Journal* **2017**, 20, 1155-1165.

64. Liu, Y.; Liu, Z.; Pan, W.; Wu, Q. Absorption behaviors and structure changes of chitin in alkali solution. *Carbohydrate Polymers* **2008,** 72, 235-239.

65. Agustin, M. B.; Nakatsubo, F.; Yano, H. The thermal stability of nanocellulose and its acetates with different degree of polymerization. *Cellulose* **2016**, 23, 451–464.

66. Chen, P-Y; Lin, A. Y-M; McKittrick, J; Meyers, M. A: Structure and mechanical properties of crab exoskeletons. *Acta Biomaterialia* **2008**, 4, 587-596.

67. Zewude, D. A.; Noguchi, T.; Sato, K.; Izawa, H.; Ifuku, S. Production of chitin nanoparticles by bottom-up approach from alkaline chitin solution. *International Journal of Biological Macromolecule* **2022**, 210, 123-127.

68. Sannan, T.; Kurita, K.; Iwakura, Y. Studies on chitin. V. kinetics of deacetylation reaction. *Polymer Journal* **1977**, 9, 649-651.

69. Ifuku, S.; Ikuta, A.; Izawa, H.; Morimoto, M.; Saimoto, H. Control of mechanical properties of chitin nanofiber film using glycerol without losing its characteristics. *Carbohydrate Polymers* **2014**, 101, 714- 717.

List of publications

1. Zewude, D.A.; Izawa, H.; Ifuku, S. Optimum preparation conditions for highly individualized chitin nanofibers using ultrasonic generator. *Polymers* **2021**, 13, 2501. [Chapter 1]
2. Zewude, D.A.; Izawa, H.; Ifuku, S. Optimization of chitin nanofiber preparation by ball milling as filler for composite resin. *Journal of composite science* **2022**, 6, 197. [Chapter 2]
3. Zewude, D.A; Noguchi, T.; Sato, K.; Izawa, H.; Ifuku, S. Production of chitin nanoparticles by bottom-up approach from alkaline chitin solution. *International journal of biological macromolecule* **2022**, 210, 123-127. [Chapter 3]
4. Zewude, D.A; Noguchi, T.; Sato, K.; Izawa, H.; Ifuku, S. Preparation of partially deacetylated chitin nanoparticles by bottom-up approach. *Chitin and chitosan research* **2022,** 28(1), 10-15. [Chapter 4]

Acknowledgements

Throughout my study time I have received a great deal of support. I would like to offer my deepest appreciations to all who have played a role.

I would like to express my sincere gratitude and special thanks to my supervisor professor Shinsuke Ifuku for guidance, advise, and mentoring. I feel extremely lucky for studying under your supervision. The experience and lesson that I have got from you heightens me in the next part of my academic career.

I would like to extend my deepest gratitude to Professor Hironori Izawa for encouraging and guiding me in the right direction. The comments and suggestions that you have forwarded has taught me a lot and made our contribution stronger. I am extremely grateful to all members of the Ifuku Laboratory for constant support and assistance.

I am deeply indebted to the Government of Japan, Ministry of Education, Culture, Sport, Science, and Technology (MEXT) for complete financial support to achieve higher education and experience Japanese culture.

My heart can’t thank enough my mother Aylech Hundie for love and affection I received. Your love has made me strong and helped me to pass through many challenges. My mother you are so strong and determined. When life challenges me, I always remember your life journey. It gives me energy. You have kept a unique love and view of life in my mind and heart.

I have special gratitude for my father late Abebe Zewude for the love you shared me and the discipline you thought me. Even if you left me very early, I remember most of the moments I had with you and I always think you are with me.

I have special thanks to my wife Meseret Gutema. Your constant love and patience gave me strength to finish this study. I would like to thank my little baby Maya Dagmawi. You have changed my views in life and become the reason of hope. Now, I believe tomorrow is always there.

I would like to thank my brother, sister, relatives and friends for your support and encouragement while I am passing through several ups and downs.